

# 1        **Extrapolating regional probability of drying of headwater streams**

## 2                    **using discrete observations and gauging networks**

3        **Aurélien BEAUFORT**<sup>1</sup>, Nicolas LAMOUREUX<sup>1</sup>, Hervé PELLA<sup>1</sup>, Thibault DATRY<sup>1</sup> and Eric SAUQUET<sup>1</sup>

4        <sup>1</sup>Irstea, UR RiverLy, centre de Lyon-Villeurbanne, 5 rue de la Doua CS 20244, 69625 Villeurbanne,  
5        France

### 6        **Abstract**

7        Headwater streams represent a substantial proportion of river systems and many of them have  
8        intermittent flows due to their upstream position in the network. These intermittent rivers and  
9        ephemeral streams have recently seen a marked increase in interest, especially to assess the impact  
10       of drying on aquatic ecosystems. The objective of this paper is to quantify how discrete (in space and  
11       time) field observations of flow intermittence help to extrapolate over time the daily probability of  
12       drying (defined at the regional scale). Two empirical models based on linear or logistic regressions  
13       have been developed to predict the daily probability of intermittence at the regional scale across  
14       France. Explanatory variables were derived from available daily discharge and groundwater level data  
15       of a dense gauging/piezometer network, and models were calibrated using discrete series of field  
16       observations of flow intermittence. The robustness of the models was tested using (1) an  
17       independent, dense regional data set of intermittence observations, (2) observations of the year  
18       2017 excluded from the calibration. The resulting models were used to extrapolate the daily regional  
19       probability of drying in France: (i) over the period 2011-2017 to identify the regions most affected by  
20       flow intermittence; (ii) over the period 1989-2017, using a reduced input dataset, to analyze  
21       temporal variability of flow intermittence at the national level. The two empirical regression models  
22       performed equally well between 2011 and 2017. The accuracy of predictions depended on the  
23       number of continuous gauging/piezometer stations and intermittence observations available to  
24       calibrate the regressions. Regions with the highest performance were located in sedimentary plains,

25 where the monitoring network was dense and where the regional probability of drying was the  
26 highest. Conversely, worst performances were obtained in mountainous regions. Finally, temporal  
27 projections (1989-2016) suggested highest probabilities of intermittence (> 35%) in 1989-1991, 2003  
28 and 2005. A high density of intermittence observations improved the information provided by  
29 gauging stations and piezometers to extrapolate the temporal variability of intermittent rivers and  
30 ephemeral streams.

31 **Keywords:** Intermittent rivers, headwater streams, flow regime, discrete observations, regional scale

## 32 **1. Introduction**

33 Headwater streams represent a substantial proportion of river systems (Leopold et al., 1964; Nadeau  
34 and Rains, 2007; Benstead and Leigh, 2012). From an ecological point of view, headwater catchments  
35 are at the interface between terrestrial and aquatic ecosystems and they often harbour a unique  
36 biodiversity with a very high spatial turn-over (Meyer et al., 2007; Clarke et al., 2008; Finn et al.,  
37 2011). Their contribution to the functioning of hydrographic networks is essential: sediment flows,  
38 inputs of particulate organic matter and nutrients, refugia/colonization, sources for aquatic  
39 organisms (Meyer et al., 2007; Finn et al., 2011).

40 Headwater streams are generally naturally prone to flow intermittence, i.e. streams which stop  
41 flowing or dry up at some point in time and space, mainly due to their upstream position in the  
42 network and their high reactivity to natural or human disturbances (Benda et al., 2005; Datry et al.,  
43 2014b). These waterways which cease flow and/or dry are referred to as intermittent rivers and  
44 ephemeral streams (IRES). The geographic extent of IRES is poorly documented due to mapping  
45 limitations (digital elevation models, satellite images, aerial photos) and because of their size and  
46 their location (Leopold et al., 1994; Nadeau and Rains, 2007; Benstead and Leigh, 2012; Fritz et al.,  
47 2013). However the proportion of IRES in hydrological networks can be very large: for example, they  
48 represent 60% of the length of rivers in the United States (Nadeau and Rains, 2007) and are

49 considered to represent probably more than 50% of the global hydrological network (Larned et al.,  
50 2010; Datry et al., 2014b). Considering only gauging stations with continuous records may lead to  
51 severe underestimation of their regional extent (Snelder et al., 2013; De Girolamo et al., 2015; Eng et  
52 al., 2016).

53 Recently, IRESs have seen a marked increase in interest stimulated by the challenges of water  
54 management facing the global change context (water scarcity issues, climate change impact, etc.)  
55 (Acuña et al., 2014; Datry et al., 2016b). Studies have characterized the hydrological functioning of  
56 IRES (Gallart et al., 2012; Costigan et al., 2016; Sarremejane et al., 2017) to assess the effects of flow  
57 intermittence on aquatic ecosystems (Larned et al., 2010; Datry et al., 2016b; Leigh et al., 2016; Leigh  
58 and Datry, 2017). IRES have been altered due to human actions (abstraction, hill dams, low-water  
59 support, pollution, etc.) despite their high and unique biodiversity (Datry et al., 2014; Garcia et al.,  
60 2017a). In addition, some perennial streams are becoming intermittent due to global change, water  
61 abstraction or river damming (Skoulikidis, 2009) and the extent of IRES may increase in the future  
62 (Döll and Schmied, 2012; Jaeger et al., 2014; Pumo et al., 2016; Garcia et al., 2017b; De Girolamo et  
63 al., 2017).

64 A better hydrological understanding of IRES is now essential and an improved management requires  
65 knowing both the spatial extent and arrangement of IRES within the river network (Boulton, 2014;  
66 Acuña et al., 2017). Efforts have been made to estimate the spatial distribution of IRES at the  
67 catchment scale (Skoulikidis et al., 2011; Datry et al., 2016a), at the regional scale (Gómez et al.,  
68 2005) and at the national scale (Snelder et al., 2013). In France, Snelder et al. (2013) suggested a  
69 classification of IRES regimes and spatialized their distribution. Based on an analysis of the  
70 continuous gauging network, they showed that the proportion of IRES accounted for 20 to 39% of the  
71 hydrographic network. The accuracy of the obtained map is highly dependent on the density of the  
72 flow monitoring network. The installation of additional gauging stations is expensive and headwaters  
73 systems may be difficult to monitor due to active geomorphology processes or to difficult access.

74 As a promising tool to advance the mapping of IRES, citizen science creates opportunities to  
75 overcome the lack of hydrological data and contributes to densify the flow state observation network  
76 (Turner and Richter, 2011; Buytaert et al., 2014; Datry et al., 2016b) and could be used for  
77 hydrological model calibration (van Meerveld et al., 2017). In France, Datry et al. (2016a) used such  
78 data to describe the spatiotemporal dynamics of aquatic and terrestrial habitats within five river  
79 catchments located in the western part of France. They showed that processes resulting in flow  
80 intermittence were complex at a fine scale and could vary substantially among nearby catchments.  
81 However, these data were only available in a few catchments, limiting any attempt to map large-  
82 scale patterns of flow intermittence in river networks. Since this first attempt, new sources of  
83 observational data have become available in France thanks to the ONDE network (Observatoire  
84 National des Etiages, <https://onde.eaufrance.fr>). This unique network in Europe provides frequent  
85 discrete field observations (five inspections per year) of the flow intermittence across more than 3  
86 300 sites throughout France and located mostly in headwater areas.

87 However discrete observations of intermittence do not provide any information on the persistence of  
88 dry conditions between two consecutive dates of observation. The rewetting-drying events could  
89 have significant impacts on communities whose survival is conditioned by the duration/frequency of  
90 drying. The duration of drying is of importance for ecologists, as one key driver for the composition  
91 and persistence of aquatic species (Vardakas et al., 2017; Kelso and Entrekkin, 2018, Vadher et al.,  
92 2018). Temporal extrapolations of river flow regime are thus necessary to summarize the different  
93 facets of flow intermittence at various time scales, from daily to inter-annual.

94 The main objective of this paper is to use discrete (in space and time) field observations of flow  
95 intermittence to extrapolate over time the daily probability of drying (averaged at the regional scale).  
96 We first carried out a quantitative analysis of the ONDE network data in order to characterise the  
97 information that they contribute in comparison with the data resulting from the conventional  
98 hydrological monitoring. Then, we developed two empirical models based on linear or logistic

99 regressions to convert discontinuous series of flow intermittence observation from ONDE into  
100 continuous daily probability of drying, defined at the regional scale across France. Explanatory  
101 variables were derived from available continuous daily discharge and groundwater level data of a  
102 dense gauging/piezometer network, and models were calibrated using the ONDE discrete  
103 observations. The robustness of the models was tested using (1) an independent, dense regional data  
104 set of intermittence observations and (2) observations of the year 2017 excluded from the  
105 calibration. Finally, resulting models were used to extrapolate the regional probability of drying in  
106 France: (i) over the period 2012-2017 to identify the regions most affected by flow intermittence; (ii)  
107 over the period 1989-2017, using a reduced input dataset, to analyze temporal variability of flow  
108 intermittence at the national level.

## 109 **2. Material and Methods**

### 110 **2.1. Study area**

111 The study area is continental France and Corsica (550 000 km<sup>2</sup>). France is located in a temperate zone  
112 characterized by a variety of climates due to the influences of the Atlantic Ocean, the Mediterranean  
113 Sea and mountain areas.

114 We defined regions as combinations of "level-2 Hydro-EcoRegions" (HER2) and classes of  
115 hydrological regimes (HR). Hydro-EcoRegion (HER) corresponds to a typology developed for river  
116 management in accordance with the European Water Framework Directive. The Hydro-EcoRegion  
117 classification includes 22 "level-1 Hydro-EcoRegions " (HER1) based on geology, topography and  
118 climate, and considered as the primary determinants of the functioning of water ecosystems  
119 (Wasson et al., 2002). HER2 correspond to a finer classification accounting for stream size. HER2 have  
120 a mean drainage area of 5 000 km<sup>2</sup> (between 100 and 27 000 km<sup>2</sup>). The hydrological regimes classes  
121 (HR) were identified by reference to the work carried out by (Sauquet et al., 2008) where it was  
122 possible to distinguish rainfall-fed regimes, transition and snowmelt-fed river flow regimes. Overall,

123 we used 280 regions (that is, HER2-HR combinations) with a mean drainage area of 1 400 km<sup>2</sup>  
124 (between 4 and 20 000 km<sup>2</sup>).

## 125 2.2. ONDE dataset discrete national flow-state observations

126 The ONDE network was set up in 2012 by the French Biodiversity Agency (AFB, formerly ONEMA)  
127 with the aim of constituting a perennial network recording summer low flow levels and used to  
128 anticipate and manage water crisis during severe drought events (Nowak and Durozoi, 2012).

129 There are 3 300 ONDE sites distributed throughout France (Fig. 1). ONDE sites are located on  
130 headwater streams with a Strahler order strictly less than 5 and balanced across HER2 regions to take  
131 into account the representativeness of the hydrological contexts (Nowak and Durozoi, 2012). The  
132 ONDE network is stable over time. Observations are made monthly (around the 25<sup>th</sup>) by trained AFB  
133 staff, between April and September, every year since 2012. One of the statuses is assigned at each  
134 observation among “visible flow”, “no visible flow” and “dried out”. Here, we consider two  
135 intermittency statuses: “**Flowing**” when there is visible flow across the channel (“visible flow”) and  
136 “**Drying**” when the channel is entirely devoid of surface water (“dried out”) or when there is still  
137 water in the river bed but without visible flow (disconnected pools, lentic systems) (“no visible  
138 flow”). The proportion of drying sites determined on the basis of the ONDE network for each HER2-  
139 HR combination is considered as a good estimate of the daily Regional Probability of Drying  
140 (RPOD<sub>ONDE</sub>) of streams with a Strahler order less than 5. Observed values of RPOD<sub>onde</sub> are calculated as  
141 follows:

$$142 \quad RPOD_{ONDE}(d) = \frac{(Ndrying)_{HER2-HR}}{(Nflowing + Ndrying)_{HER2-HR}} \quad (1)$$

143 where  $d$  denotes the observation date of the ONDE network,  $Ndrying$  and  $Nflowing$  are the number  
144 of drying and of flowing statuses observed at ONDE sites located in a same HER2-HR combination at  
145 the observation date  $d$ , respectively.

146 Figure 2 illustrates the complementary nature of the ONDE network to the already existing French  
147 river flow monitoring network HYDRO (<http://www.hydro.eaufrance.fr>). The ONDE sites and a set of  
148 1 600 gauging stations available in the HYDRO database have been projected on the river network  
149 RHT (Theoretical Hydrographic Network; Pella *et al.*, 2012) and the drainage area and the elevation  
150 have been estimated. A large part of ONDE sites are located on small headwater streams with 70% of  
151 the sites with a drainage area of less than 50 km<sup>2</sup> while most of the gauging stations record flows of  
152 catchments of medium size (between 100 and 500 km<sup>2</sup>). Only four stations display a drainage area of  
153 more than 1 000 km<sup>2</sup>. The distributions of elevation of the two databases look similar. The ONDE  
154 sites are mostly located on rivers with an elevation below 200 m (75% of sites). The ONDE sites are  
155 sparse at high elevations (95 sites located above 1 000 m). This bias is likely due to access difficulties  
156 in mountainous areas.

### 157 **2.3. POC dataset: a denser regional dataset used for independent** 158 **validation**

159 A spatially denser citizen science dataset of flow-state observations in western France (Poitou-  
160 Charente region) (<http://atlas.observatoire-environnement.org>) has been used as validation dataset  
161 to test the robustness of our models calibrated with the ONDE dataset. The POC monitoring (2011-  
162 2013) covered more than 4 000 km of river length across 20 catchments. Each river was entirely  
163 surveyed every 1<sup>st</sup> and 15<sup>th</sup> of each month between June and October, resulting in eight observations  
164 per year. Four intermittency statuses were available in the POC dataset (Datry *et al.* 2016a) but to  
165 allow comparisons with the ONDE network, we pooled the two “Flowing” and “Low Flow” POC  
166 statuses into a single “**Flowing**” status and the two “No flow” and “Dry” statuses into the “**Drying**”  
167 status. This dataset is available as maps with flow states assigned to the inspected streams. Values of  
168 RPoD at each POC observation date is calculated in the same way as RPoD<sub>ONDE</sub>. Thus RPoD<sub>POC</sub> is given  
169 by the ratio between the number of drying statuses and the total number of observations at each  
170 inspected streams located in a same HER2-HR.

## 171        **2.4. Explanatory discharge dataset**

172        Two discharge datasets (continuous daily time series) were used as explanatory variables of discrete  
173        intermittence observations, with the objective of extrapolating the intermittence frequency over  
174        time. The two datasets included time series of daily discharge extracted from the French River  
175        discharge monitoring network ("HYDRO database", <http://www.hydro.eaufrance.fr/>): (i) **the 2011-**  
176        **2017 dataset** with full records available between the 01/01/2011 and 31/06/2017; (ii) **the 1989-2017**  
177        **dataset** concerning a reduced number of gauging stations and providing daily discharges between  
178        the 01/01/1989 and 31/06/2017. According to the hydrometric services in charge of the selected  
179        gauging stations, high quality of measurements was ensured and observed discharges were not or  
180        only slightly altered by human actions.

181        The 2011-2017 dataset was composed of 1 600 gauging stations distributed across France. Each  
182        stream where a HYDRO gauging station is located has been defined as IRES or perennial. Several  
183        definitions of IRES can be found in the literature (Huxter and van Meerveld, 2012, Eng et al., 2016;  
184        Reynolds et al., 2015). In this study, we considered stations as intermittent when five consecutive  
185        days with discharge less than 1 liter per second has been observed during the period of record.

186        The 1989-2017 dataset consisted of 630 gauging stations selected with less than 5% of missing data  
187        (continuous or not) during the period 1989-2017. This dataset has been thereafter used to estimate  
188        the regional probability of drying before the creation of the ONDE network.

## 189        **2.5. Explanatory groundwater level dataset**

190        Because groundwater resources influence stream intermittence, we used available time series of the  
191        daily groundwater level available in the ADES database (<http://www.adès.eaufrance.fr/>) at sites  
192        identified as involved in groundwater/surface water exchanges (Brugeron et al., 2012). Similarly to  
193        the discharge data, two sets of groundwater level data with records available over the two periods  
194        2011-2017 and 1989-2017 have been selected. The level of alteration of groundwater levels by water  
195        withdrawal is unknown because no information is available at this scale.



196 The 2011-2017 dataset was composed by 750 piezometers with daily groundwater level data with  
 197 less than 5% of missing data (continuous or not). The selection of 1989-2017 dataset was not easy  
 198 because few groundwater level measurements were available in the database before 2000. For  
 199 example, only five piezometers met the tolerance limit on missing values considered for the 1989-  
 200 2017 discharge dataset. In order to extend the dataset and because groundwater levels were less  
 201 variable than stream discharges, the proportion of permitted gaps was fixed to 20% between 1989  
 202 and 2017. This led us to select 150 piezometers. Thereafter, when the missing data period was less  
 203 than 10 days, groundwater levels were reconstructed by linear interpolation in order to reduce the  
 204 proportion of missing values to less than 5% for the 150 piezometers selected.

## 205 **2.6. Statistical modeling of regional probability of drying**

206 The parametric modeling strategy was based on 5 main steps (Fig. 3). The first step consisted in  
 207 selecting all ONDE sites, gauging stations and piezometers located in a same HER2-HR combination.  
 208 When the total number of gauging stations and piezometers was less than 5 for a HER2-HR  
 209 combination, we merged the HER2-HR combination with a neighboring one located in the same  
 210 HER1. This was done for 20 of the 280 regions. The second step consisted in calculating the  $RPOD_{ONDE}$   
 211 for each observation date (5 per year) and for all selected ONDE sites. In a third step, a flow duration  
 212 curve was determined for each selected HYDRO gauging station. The average non-exceedance  
 213 frequency of the observed discharge at gauging stations was averaged for the date of observation (d)  
 214 at ONDE sites and the 5 days preceding the observation. The lag of six days accounted for the fact  
 215 that ONDE survey dates in a region could differ by 5 days, and accounted for the inertia of physical  
 216 processes (e.g. storage capacity). The same operation was carried out with selected piezometers.  
 217 Finally the hydrological conditions are described by the average (across stations) F of the non-  
 218 exceedance frequencies of discharge (Fq) and groundwater levels (Fgw) with respect to the relative  
 219 proportions of gauging stations and piezometers:

$$220 \quad F(d) = \frac{\sum_{i=1}^{i=Nq} Fq_i + \sum_{j=1}^{j=Ngw} Fgw_j}{(Nq + Ngw)} \quad (2)$$

221 Where  $F_{qi}$  denotes the average non-exceedance frequency of discharge at the gauging station  $i$   
 222 calculated between  $d$  and  $d-5$ ;  $F_{gwj}$  the average non-exceedance frequency of groundwater levels at  
 223 the piezometer  $j$  calculated between  $d$  and  $d-5$ ;  $N_q$  the number of gauging stations selected in a  
 224 HER2-HR combination and  $N_{gw}$  the number of selected piezometers selected in the HER2-HR  
 225 combination. The fourth step consisted in estimating the  $RPoD_{ONDE}$  as a function of  $F$ . Two types of  
 226 regression were fitted for each HER2-HR combination across France:

227 a truncated logarithmic linear regression (LLR), with two parameters  $\alpha_1$  and  $\beta_1$ :

$$228 \quad RPoD_{LLR}(d) = \begin{cases} \min(1; \alpha_1 \times \ln(F(d)) + \beta_1) & \text{when } F < F_0 \\ 0 & \text{when } F \geq F_0 \end{cases} \quad (3)$$

229  $F_0$  was fixed as the value of non-exceedance frequencies of discharge and groundwater levels at  
 230 which no more drying status was observed across the ONDE network ( $RPoD_{ONDE} = 0$ ).

231 a logistic regression (LR), with two parameters  $\alpha_2$  and  $\beta_2$ :

$$232 \quad \text{Logit}(RPoD_{LR}(d)) = \ln\left(\frac{RPoD_{LR}(d)}{1-RPoD_{LR}(d)}\right) = \alpha_2 \times F(d) + \beta_2 \quad (4)$$

233 LR is a multivariate analysis method well known for its relevance in binary classification issues (Lee,  
 234 2005). The  $RPoD_{LR}$  was then calculated as following Eq. 5:

$$235 \quad RPoD_{LR}(d) = \frac{\exp(\alpha_2 + \beta_2 F(d))}{1 + \exp(\alpha_2 + \beta_2 F(d))} \quad (5)$$

236 Models were calibrated against observations available during the same period, 2012-2016, leaving  
 237 out the year 2017 for an independent validation test. However, for the continuous temporal  
 238 extrapolations (one over 2011-2017, the other 1989-2017), two models were built with different  
 239 piezometers and gauging stations selected as explanatory variables (see section 2.4 and 2.5). Thus  
 240 there are two sets of regressions parameters specific to each dataset for both LLR and LR models  
 241 leading to different prediction of  $RPoD$ .

242 Finally, in a fifth step, a daily regional probability of drying (RPoD) could be predicted for each HER2-  
 243 HR combination with both models following analytical formulas (Eq. 3 and Eq. 5).

## 244 **2.7. Model robustness: validation using independent data sets**

245 We used (1) the POC independent data and (2) the 2017 ONDE year to test the robustness of the LLR  
 246 and LR model to predict the intermittence frequency (1) in space and (2) over time. Note that when  
 247 predicting on the POC datasets, a new model was calibrated using only ONDE sites located out of  
 248 POC streams.

249 For both datasets (POC and ONDE 2017), the relative performance of the LLR and LR models was  
 250 compared in multiple ways using both the 2011-2017 and the 1989-2017 datasets. The performance  
 251 of each model was evaluated by the Nash-Sutcliffe efficiency criterion (NSE) (Nash and Sutcliffe,  
 252 1970):

$$253 \quad NSE = 1 - \frac{\sum_{i=1}^N (RPoD_{ONDEi} - RPoD_{pri})^2}{\sum_{i=1}^N (RPoD_{ONDEi} - \overline{RPoD_{ONDEi}})^2} \quad (6)$$

254 where  $RPoD_{ONDEi}$  is the average proportion of drying statuses over the ONDE sites located in the  
 255 HER2-HR combination at the  $i^{th}$  observation date,  $RPoD_{pri}$  is the predicted regional probability of  
 256 drying at the  $i^{th}$  observation date,  $\overline{RPoD_{ONDEi}}$  is the mean of  $RPoD_{ONDEi}$  over the period and  $N$  is the  
 257 total number of observations in the ONDE network for each HER2-HR combination.

## 258 **2.8. Model prediction**

259 Both models have been calibrated over the period 2012-2016 and were then applied in a 5<sup>th</sup> step to  
 260 predict the daily RPoD in France (Fig. 3). The RPoD was firstly predicted over the period 2012-2016 in  
 261 order to identify the most affected regions by flow intermittence using the 2011-2017 datasets. The  
 262 second application concerned the extrapolation of RPoD in France over a longer period using the  
 263 1989-2017 dataset to analyze the temporal variability of flow intermittence at the national level. It

264 should be noted that model predictions only concern streams with a Strahler order lower than 5 due  
265 to the ONDE sites location.

## 266 **3. Results**

### 267 **3.1. Quantitative analysis**

#### 268 **3.1.1. Inter-annual intermittence according to the raw discrete ONDE network**

269 A total of 1 127 ONDE sites have recorded at least one drying event during the period 2012-2016  
270 representing 35% of the 3 300 ONDE sites. From the ONDE database the probability of drying at the  
271 country scale was computed as the total number of drying statuses over France divided by the total  
272 number of ONDE observations available during statuses the same year (Fig. 4a). Between 2012 and  
273 2016, the most critical year is 2012 with 15% of drying statuses followed by 2016 (14%) and 2015  
274 (14%) (Fig. 4a). The years 2013 and 2014 are less affected with only 6% of drying statuses observed  
275 (Fig. 4a).

276 Drying events mainly occur between July and September but the evolution of the month's proportion  
277 of drying can differ between years (Fig. 4b). In more detail, water levels in 2012 decrease in August  
278 when the proportion of drying is 27% and the situation lasts until the end of September with 25% of  
279 drying (Fig. 4b). In 2013, the proportion of drying is lower than in 2012 but follows the same pattern  
280 with an increase at the end of July (3%) and reaching 9% in August and in September. In 2014, the  
281 first peak of drying (5%) is reached early in June. Then, the proportion of drying decreases in July  
282 (3%) and increases slightly in August 4% and reaching 7% in September. In 2015, the critical period  
283 occurs at the end of July with 19% of drying statuses and the proportion of drying decreases slightly  
284 at the end of August (17%) until it reaches 9% in September. Finally, in 2016, the situation is  
285 gradually deteriorates every month, reaching 20% of drying statuses in August, and 28% in  
286 September.

287 Between 2012 and 2016, a proportion of drying higher than 50% is recorded on 93 ONDE sites and  
288 their spatial distribution is very patchy at the France scale (black and dark grey dots, Fig. 5a). There  
289 are only 158 ONDE sites with at least one drying event every year and a variability of drying locations  
290 can be observed across years. The south-east of France is heavily affected by rivers drying where the  
291 proportion of drying can exceed 75% annually (black dots, Fig. 5b-5f). The north-western part of  
292 France is less affected, although many ONDE sites show a proportion of drying observed above 50%  
293 in 2014 and 2016 (Fig. 5d and 5f). Northeastern France is rather affected in 2012, 2014 and 2015  
294 where several ONDE sites have more than 75% of drying statuses (Fig. 5b, 5d and 5e). The south-west  
295 France is particularly affected in 2012 and 2015 (Fig. 5b and 5e).

### 296 **3.1.2. Comparison of flow intermittence between the raw ONDE and HYDRO datasets**

297 The HYDRO dataset includes 90 gauging stations located on streams considered as IRES, which  
298 represents only 5.6% of the 1 600 gauging stations against 35% for ONDE sites. At the national scale,  
299 the number of IRES seems underrepresented in the south-western, central, northeastern part of  
300 France and Corsica in comparison with sites experiencing drying in the ONDE network (Fig. 6).

301 The number of gauging stations with at least one drying event (discharge < 1 l/s) observed between  
302 May and September varies between 79 in 2012 and 47 in 2014 (Table 1). The lowest numbers of  
303 gauging stations with drying events are observed in the years 2013 and 2014 while the highest  
304 numbers are related to the years 2012, 2015 and 2016. This finding is consistent with the analysis of  
305 the ONDE network (Fig. 5a, d). The frequency of drying, corresponding to the ratio between the  
306 number of dry days and the total number of days between the 1<sup>st</sup> May and the 30<sup>th</sup> September (153  
307 days), in contrast, is quite constant over the years (~30%). The number of gauging stations with  
308 drying event over more than 50% of the time varies little between wet years (14 in 2013) and dry  
309 years (21 in 2015) unlike ONDE observations, suggesting a significant temporal variability in the  
310 frequency of drying between dry and wet years (Fig. 5).

## 311        **3.2. Validation of the predicted regional probability of drying**

### 312        **3.2.1. Regression results**

313 LLR and LR models, calibrated over the period 2012-2016, perform well with the 2011-2017 dataset  
314 with a mean NSE of 0.8 with LR model against 0.7 with LLR model (Fig. 7a and b). With the LR model,  
315 50% of the HER2-HR combinations obtain a NSE greater than 0.8, representing a coverage of 65% of  
316 the French territory, while 33% of HER2-HR combinations display a NSE higher than 0.8 (50% of  
317 France coverage) with the LLR model. Regions with the highest performances are located in  
318 sedimentary plains, in the south-east of France and in the Pyrenees Mountains. Conversely, the  
319 worst performances are obtained in the mountainous regions of Alps as well as in the Massif Central.  
320 In these regions the size of the HER2 is rather small and the number of ONDE sites, gauging stations  
321 and piezometers per HER2-HR combinations are certainly too few to derive reliable relations. Despite  
322 pooling, estimating RPoD remains impossible for 9 HER2-HR combinations (4.5% of France coverage)  
323 because the number of ONDE sites, gauging stations and piezometers sites is insufficient (less than 5)  
324 to perform the regression analysis.

325 The performance level is lower when the 1989-2017 dataset is used in models: the mean NSE with  
326 the LR and LLR models is 0.7 and 0.6, respectively (Fig. 7c and d).

327 The LR and LLR models lead to similar performance range. However, the LR model outperforms the  
328 LLR model in terms of number of HER2-HR combinations with NSE greater than 0.8 (Fig. 7c and d).

329 The performance is sensitive to the dataset. As expected, the best results are obtained with the  
330 denser network. A decrease in NSE by more than 0.2 is identified for 5% of the French territory when  
331 the 1989-2017 dataset is used (black areas; Fig. 7e and f). The regions with the most degraded values  
332 of NSE are small HER2-HR combinations located in eastern France (Fig. 7e and f).

333 The decrease in performance is mainly due to the difference in number of gauging stations and  
334 piezometers between the two datasets (Fig. 8). The most degraded NSEs correspond to HER2-HR

335 combinations where the number of gauging stations and piezometers considered in regressions is  
336 the most reduced, i.e. with a loss higher than 50% of stations (black and dark grey dots; Fig 8a and b).  
337 However, the decrease in performance remains low (difference in NSE is below 0.1 for 75% and 64%  
338 of HER2-HR combinations with LLR and LR model, respectively).

### 339 **3.2.2. Comparison to the POC database**

340 The observed proportion of drying  $RPoD_{POC}$  is rather well simulated by both LLR and LR models with  
341 the 2011-2017 explanatory dataset ( $NSE > 0.7$  except for the year 2011, Fig. 9). In addition, the  
342 models are able to capture small fluctuations of  $RPoD_{POC}$  during the summer period. The best results  
343 during the year 2011 are obtained with the LLR model (black curve; Fig. 9) and the LR model  
344 overestimates  $RPoD_{POC}$  by 3% (dashed grey curve; Fig. 9). In 2012, the decline in water levels is more  
345 gradual than in 2011 and a marked peak is reached in September with 40% of  $RPoD_{POC}$  (Fig. 9). This  
346 pattern is well reproduced by both models with a good fit to all observation points (Fig. 9). The year  
347 2013 is less affected by drying occurrence and the maximum  $RPoD_{POC}$  does not exceed 20% (Fig. 9).  
348 Curves of both models fit to observations well until the end of August. Note that the LR model is  
349 slightly closer to the observations around the peak in September compared to the LLR model.  
350 However the LR model overestimates the  $RPoD_{POC}$  at the end of September and in October.  
351 When the 1989-2017 dataset is used as explanatory variables, the simulations of  $RPoD$  are weakly  
352 degraded with both models (Fig. 9d, e, f). However the simulated pattern is similar to the observed  
353 one. The LLR model outperforms the LR model during the three years of validation with the 1989-  
354 2017 dataset (black curve; Fig. 9d, e, f).

### 355 **3.2.3. Temporal patterns assessment of models between 2012 and 2017**

356 During the calibration period, the LLR and LR models tend to better simulate the  $RPoD$  during dry  
357 years 2012 and 2016 ( $NSE = 0.8$  with LLR and LR models; Tab. 2) than during wet years (e.g. 2014 with  
358  $NSE < 0.7$ ). The NSEs are lower during the months of May and June when few drying events are  
359 observed while NSEs are much better during the driest months of August and September.

360 During the validation year of 2017, both models obtain a similar performance over the year  
361 independent of datasets (NSE = 0.7).

362 Monthly NSEs in 2017 follow the same trend as monthly NSEs of the calibration period with lower  
363 NSEs in May (NSEs < 0.4) and June (NSEs = 0.5) and higher NSEs in July, August and September (NSEs  
364 = 0.6) with both models independent of datasets. Figure 10 shows the dispersion between predicted  
365 RPOD and drying statuses observed at ONDE sites in the scatter plot during the validation year 2017  
366 (Fig. 10a and 10b) in comparison with the year 2012 which obtains the better NSE during calibration  
367 period (Fig. 10c and 10d). The NSEs obtained in 2017 are 0.72 with the LLR model and 0.68 with the  
368 LR model against 0.83 and 0.81 in 2012, respectively. The performance is slightly lower in 2017 but  
369 remains acceptable with NSEs close to 0.7 and both models seem able to predict RPOD out of the  
370 calibration period.

### 371 **3.3. Application of regional models**

#### 372 **3.3.1. Modeling of intermittencies severity between 2012 and 2016**

373 Both models have been applied using the 2011-2017 dataset. Figure 11 displays the maximum  
374 number of consecutive days ( $D_{\text{RPOD}>20\%}$ ) with RPOD higher than 20% simulated by both LLR and LR  
375 models. The most affected regions are located in the south-east of France and in the sedimentary  
376 plains which are consistent with the spatial pattern obtained from the ONDE observations (Fig. 5).  
377 The most impacted year followed the same hierarchy: the year 2012 is the most critical year with  
378 30% of France displaying  $D_{\text{RPOD}>20\%}$  higher than 60 days followed by the year 2015 (20% of France with  
379  $D_{\text{RPOD}>20\%} > 60$  days) and 2016 (15% of France with  $D_{\text{RPOD}>20\%} > 60$  days) (Fig. 11). The years 2013 and  
380 2014 are weakly affected with 5% and 6% of the France with  $D_{\text{RPOD}>20\%}$  higher than 60 days,  
381 respectively.



382 The LR model tends to simulate shorter periods of drying, particularly in HER2-HR combinations  
383 located in the South-East France in 2013 and 2014 (Fig. 11). However, there is an overall agreement  
384 between RPoD simulated by both models in terms of spatial and temporal extent of dry streams.

### 385 **3.3.2. Reconstitution of historical regional probability of drying**

386 The trend temporal patterns of RPoD predicted by the two models, considering the 1989-2017  
387 dataset, look similar between 1989 and 2016 and the simulated RPoD fit well to RPoD<sub>ONDE</sub> (Fig. 12).

388 The proportion of drying is highly variable over the total simulation period, with alternating dry (1989  
389 to 1991, 2003 to 2006, 2009 to 2012) and wet (1994 to 1995, 2000 to 2002; 2013 to 2014) phases. In  
390 spite of interannual variability, peaks of RPoD occur regularly between August and September,  
391 whether in dry years or wet years. This finding is consistent with the preeminence of rainfall fed river  
392 flow regime with low flows in summer, in France.

393 The highest values of RPoDs (above 35% over France) are observed in 1989, 1990, 1991, 2003 and  
394 2005 (black curve, Fig. 12a and b). The RPoDs simulated during these dry years are out of the range  
395 of the observed values over the calibration period (2012-2016). Estimations are thus uncertain.  
396 However, the high values of RPoD are consistent with observations reported in previous studies (e.g.  
397 Larue and Giret, 2004; Snelder et al., 2013; Caillouet et al., 2017). Conversely, the years less affected  
398 by drying are simulated in 1994, 2001 and 2014 with an average RPoD below 15% throughout the  
399 year (black curve, Figs. 12a and b).

400 Results obtained with the LLR model are more contrasted in terms of extreme values than those  
401 obtained with the LR model (Fig. 12b).

## 402 **4. Discussion**

403 *ONDE network complementarity with conventional flow monitoring network*

404 The analysis of the ONDE observations shows that the proportion of rivers undergoing drying is  
405 significantly higher (35%) than that observed with the conventional monitoring (HYDRO database,  
406 8%). This proportion although related to a short period of records 2012 and 2016 is consistent with  
407 the percentage of 39% of river segments classified as intermittent by Snelder et al. (2013). This  
408 analysis confirms the under-representation of IRES in the French HYDRO database, and probably  
409 others in other countries (flow are often uncontrolled in IRES). Without gauging stations located on  
410 headwaters, Snelder et al. (2013) were unable to predict IRES in eastern France (see Fig. 9, pp. 2694).  
411 The high density of ONDE sites makes it possible to improve the detection of drying events and lead  
412 to better understand the spatial distribution of IRES located at the upstream extent of the  
413 hydrographic network. The ONDE network encompasses various hydrological conditions which  
414 provides a more accurate assessment of inter-annual variability, differentiating between dry years  
415 (2012, 2015 and 2016) and wet years (2013, 2014) with clearly few drying occurrences.

416 The validation of the LR and LLR models against the spatially dense POC database also demonstrates  
417 the spatial representativeness of the ONDE network. Thanks to the qualitative information provided  
418 and to models such as statistical models developed here, it is now possible to capture drying event at  
419 the regional scale.

420 The ONDE sites are located on small headwater streams which can be very reactive to external  
421 disturbances (rainfall deficit, change in air temperature, increase in water withdrawals, etc.) and by  
422 nature are more likely to be IRES. The gauging stations available in the HYDRO database are located  
423 on larger streams and their hydrologic response to changes in external factors (environmental or  
424 human) is slower and drying occurred with greater inertia under temperate climate. Their uneven  
425 distribution across France does not allow to accurately characterize the inter-annual variability of  
426 drying development. Overall, the ONDE network provides very complementary information to  
427 conventional flow monitoring, leading to a better understanding of the processes of drying in  
428 upstream catchments.

429 *Dependency on spatial gauging networks density*

430 The performance obtained with the LR and LLR models is slightly better with the 2011-2017 dataset  
431 (mean NSE = 0.75) than those obtained with the 1989-2017 dataset (mean NSE > 0.65), whose  
432 network is less dense. HER2-HR combinations are the most degraded where the number of  
433 monitoring stations is the most decreased between the two datasets. The accuracy of the predictions  
434 is dependent on the number of gauging stations, ONDE sites and piezometers available to calibrate  
435 the regressions. Highest NSEs are obtained in western sedimentary plains and southeastern of France  
436 where a significant number of streams have dryings regardless of years (Fig. 5). The dominant river  
437 flow regime in these regions is mainly influenced by precipitation and the lowest water levels are  
438 reached in August and September, which corresponds to the monitoring period of the ONDE  
439 database. They benefit from a dense monitoring network (gauging stations, ONDE sites,  
440 piezometers), which allows a better representation of the hydrological functioning of streams  
441 located within the same HER2. Conversely, performance was poor in mountainous areas such as in  
442 the Alps or the Massif Central (NSE < 0.4) where river flow regimes are diversified combining rainfall  
443 and snowmelt influences. By construction, the area of HER2-HR combination in mountains is  
444 reduced, which leads to a limited number of monitoring stations, certainly not sufficient to fit the  
445 models. Moreover, the observation period for ONDE sites was limited between May and September  
446 and dryings can be missed, particularly for streams influenced by snow or ice melting with potential  
447 drying periods in winter. In regions potentially concerned by drying events out of the May-September  
448 period, the actual ONDE monitoring strategy needs to be adapted to provide reliable temporal  
449 observations and extrapolations of drying frequencies.

450 We have chosen to average the non-exceedance frequencies of flows and groundwater levels in  
451 order to increase the monitoring network. If models had been calibrated using only gauging stations,  
452 performance will have been globally similar, or slightly better, in some HER2-HR combinations  
453 (Fig. 13). Therefore, we could not validate the real gain of using groundwater level data in addition to

454 discharge data. This is certainly due to the dominant proportion of the gauging stations compared to  
455 the piezometers. Indeed, in the 2011-2017 dataset, the proportion of gauging stations is greater than  
456 75% for more than 70% of HER2-HR combinations whereas the proportion of piezometers exceeds  
457 70% in only 5% of HER2-HR combinations. Groundwater level data thus have small weight in  
458 regressions for this dataset. However, in the 1989-2017 dataset, the proportion of piezometer is  
459 greater than 70% in more than 30% of HER2-HR combinations. The presence of piezometers  
460 increases the density of the monitoring network in HER2-HR combinations with few available gauging  
461 stations. Thanks to groundwater level data, RPoD can be predicted on more HER2-HR combinations.

#### 462 *Interest in reconstructing the dynamic regional probability of drying*

463 Spatio-temporal simulation of the probability of drying is crucial for advancing our understanding of  
464 IRES ecology and management. Some aquatic species can persist in a dry reach for a few days, weeks  
465 or months, while some are highly sensitive to desiccation (Datry, 2012; Storey and Quinn, 2013;  
466 Stubbington and Datry, 2013). Estimating the total duration of days with drying at the reach scale is  
467 therefore needed to understand biological patterns in river networks (Kelso and Entekin, 2018). To  
468 our knowledge, no study has proposed to reconstruct daily flow states time series of headwater  
469 streams at the country scale as France (> 500 000 km<sup>2</sup>) using discrete observations in time and space.  
470 In the literature, studies at national scale remain focused on the detection and the mapping of IRES  
471 because these rivers are historically poorly investigated and their proportion in existing hydrographic  
472 networks remains inaccurate or misunderstood (Nadeau and Rains, 2007; Snelder et al., 2013).  
473 Recently, several studies proposed alternative methodologies in order to estimate metrics in  
474 ungauged IRES (Gallart et al., 2016) or to predict daily streamflow in river basin experiencing flow  
475 intermittence (De Girolamo et al., 2017b) but remain applicable at local scale.

476 This study provides a first regional approach to use discrete data obtained from regular observations.  
477 The average non-exceedance frequency is a global hydrological statistic that only captures the  
478 hydrological conditions at the regional scale in modelling the RPoD. For rainfall-driven river flow

479 regimes, the effect of rainfall events on flow intermittence at the HER2-HR scale is probably indirectly  
480 reflected by the daily discharge and groundwater levels used to calculate the average non-  
481 exceedance frequency. However, when more observation data are available, it is likely that including  
482 more detailed descriptors of rainfall events and local geology could improve our approach. In France,  
483 based on the 2011-2017 dataset, both models suggest highest values of RPoD along the  
484 Mediterranean coast ( $D_{\text{RPoD}>20\%} > 100$  days each year). Rivers in this region are subject to a  
485 predominantly pluvial regime (Class 7; Sauquet et al., 2008), i.e. hot and dry summers follow by  
486 intense rainfall events in autumn, leading to high flows in November (Skoulikidis et al., 2017b). The  
487 catchments in this region are small and particularly reactive to environmental changes, making them  
488 highly sensitive to flow intermittence. Rivers located in the sedimentary plain in western France are  
489 also very impacted by flow intermittence. The regime is also influenced by precipitation and for the  
490 basins subject to intense agriculture significant water abstractions during summer in this region  
491 reduce water availability in rivers and in aquifers which are no longer able to support the low water  
492 levels, leading to increased flow intermittence. Regarding alteration issues in our datasets, we do not  
493 have access to the exact location and the volumes of water withdrawal for irrigation purposes.  
494 However, due to their upstream location, water availability is expected to be low, which may limit  
495 potential withdrawals and as a consequence flow alteration at ONDE sites. The alteration of  
496 groundwater levels is unknown because no information is available. However, in sedimentary plains  
497 where agricultural crops dominate the landscape, we are not sure that no human action affects low  
498 flows. It is important to note that the responses of biological communities to artificial flow  
499 intermittence is still poorly understood compared to natural IRES (Datry et al., 2014b, Skoulikidis et  
500 al., 2017a).

#### 501 *Validity of historical regional probability of drying during severe low-flow period*

502 The second application aimed at reconstructing historical RPoD over the period 1989-2016. Both  
503 models suggest highest values of mean RPoD (> 35%) in 1989-1991, 2003 and 2005. During these dry

504 years, predicted values of RPoD result from extrapolation but are consistent with published studies  
505 (Mérillon and Chaperon, 1990, Moreau, 2004). For example, Mérillon (1992) estimated that for the  
506 whole of France, 11 000 km of rivers were dried at the end of summers of 1989 and 1990. Caillouet  
507 et al (2016) found that the low-flow event observed in 1989-1990 was particularly severe in terms of  
508 duration and affected 95% of France. Snelder et al. (2013) showed from 628 gauging stations that the  
509 years 1989-1991, 2003 and 2005 had witnessed particularly high values of duration and frequency of  
510 drying events. They found that regions with the highest probability of drying were located along the  
511 Mediterranean and Atlantic coasts, which is consistent with ONDE observations and with our results.

512 Both models suggest the same sequence of dry and wet years. However the application of the LLR  
513 model lead to less contrasted RPoD than the LR model (Fig. 12).

514 To illustrate these differences, the RPoD has been simulated by both models with an extreme F of 1%  
515 (Fig. 14). The  $RPoD_{LLR}$  is significantly higher and exceeds 80% in 30% of the study area against only 5%  
516 of the area with the  $RPoD_{LR}$ . On the other hand, models simulate low RPoD in HER2-HR combinations  
517 where the  $RPoD_{ONDE}$  is very low between 2012-2016, even when F was 1% because this situation  
518 never occurred during the calibration period (Fig. 14). The logistic function of the LR model takes an  
519 S-shape which induced a decrease of the slope of the curve toward extreme values observed during  
520 the calibration period (2012-2016). The truncated logarithmic function of the LLR model is not  
521 bounded and RPoD can reach 100% during extreme low flow events by extrapolation. Since the  
522 ONDE network monitoring period does not include a period with drought as severe as in the 1990s, it  
523 is not currently possible to assess the relative performance of the two models. Refining extrapolated  
524 values requires additional information on headwater collected during more severe droughts than  
525 those observed during the last five years and then gives support to the pursuit of the ONDE network.

## 526        **5. Conclusion**

527        This paper investigates the spatial and temporal dynamics of the regional probability of drying (RPoD)  
528        of headwater streams by taking benefit from qualitative and discontinuous data provided by the  
529        ONDE network. Two models based on linear or logistic regressions have been developed and  
530        succeeded to reconstruct the temporal dynamics of RPoD. They are based on a strong relationship  
531        between the non-exceedance frequencies of discharges and groundwater levels as a function of the  
532        proportion of drying statuses observed at ONDE sites per HER2-HR combination. LLR and LR models  
533        show similar performance and perform well between 2011 and 2017. The accuracy of predictions is  
534        dependent on the number of gauging stations, ONDE sites and piezometers available to calibrate the  
535        regressions. Regions with the highest performance are located in the sedimentary plains, where the  
536        monitoring network is dense and where the RPoD is the highest. Conversely, the worst performances  
537        are obtained in the mountainous regions. Finally, both models have been used to reconstruct  
538        historical RPoD between 1989 and 2016 and suggest highest values of mean RPoD (> 35%) in 1989-  
539        1991, 2003 and 2005. This is consistent with other published studies but the high density of ONDE  
540        sites makes it possible to improve the detection of drying events and lead to better capturing of the  
541        spatial distribution of IRES located at the upstream extent of the hydrographic network. Moreover,  
542        the duration of drying is of importance for ecologists and the prediction of a daily RPoD provides one  
543        key driver for the composition and persistence of aquatic species.

544        From a methodological point of view, our method relating discrete drying observation obtained by  
545        citizen science networks to continuous daily gauging data seems robust across the highly diverse  
546        (climate and topography) regions of France, and provides good predictions in an independent region  
547        excluded from the calibration process (PoC). These two results suggest a potential application of our  
548        approach in other countries. Citizen science creates opportunities to overcome the lack of  
549        hydrological data and contributes to densify the flow state observation network (Turner and Richter,  
550        2011; Buytaert et al., 2014) and remains less expensive than the installation of additional gauging

551 stations to survey flow intermittence. The next step will be to use this regional approach to simulate  
552 the RPoD in future periods by taking into account effects of climate change through predicted  
553 discharge and groundwater level data. This would allow quantification of the evolution of the  
554 probability of drying between the current period and the different climate projections provided by  
555 the latest IPCC Report (IPCC 2014a, 2014b) and would assist decision makers in defining protocols for  
556 restoring flows with appropriate measures to preserve aquatic ecosystems (Woelfle-Erskine, 2017).

557 Secondly, further work is needed to develop an approach capable of reconstructing the drying  
558 dynamics locally by differentiating each stream. Our approach remains spatially valid to estimate  
559 RPoDs at the scale of HER2-HR combinations but does not allow characterizing the variability of  
560 drying occurrence between nearby streams within these regions. From a methodological point of  
561 view, statistical tools such as neural networks (Breiman, 2001) have shown good ability to assess  
562 both the occurrence and extent of perennial and temporary segments (González-Ferreras and  
563 Barquín, 2017) and could be investigated as an alternative method to reconstruct locally the  
564 temporal variability of drying.

## 565 **6. Acknowledgment**

566 The authors wish to thank A. van Loon and C. Sefton for their valuable comments, suggestions and  
567 positive feedback on the manuscript. The research project was partly funded by the French Agency  
568 for Biodiversity (AFB, formerly ONEMA). This study is based upon works from COST Action CA15113  
569 (SMIRES, Science and Management of Intermittent Rivers and Ephemeral Streams, [www.smires.eu](http://www.smires.eu)),  
570 supported by COST (European Cooperation in Science and Technology).



## 571 7. References

- 572 Acuña, V., Datry, T., Marshall, J., Barceló, D., Dahm, C. N., Ginebreda, A., McGregor, G., Sabater, S.,  
573 Tockner, K. and Palmer, M. A.: Why should we care about temporary waterways?, *Science*,  
574 343(6175), 1080–1081, 2014.
- 575 Acuña, V., Hunter, M. and Ruhí, A.: Managing temporary streams and rivers as unique rather than  
576 second-class ecosystems, *Biological Conservation*, 211, 12–19, doi:10.1016/j.biocon.2016.12.025,  
577 2017.
- 578 Benda, L., Hassan, M. A., Church, M. and May, C. L.: Geomorphology Of Steepland Headwaters: The  
579 Transition From Hillslopes To Channels<sup>1</sup>, *Journal of the American Water Resources Association*,  
580 41(4), 835, 2005.
- 581 Benstead, J. P. and Leigh, D. S.: An expanded role for river networks, *Nature Geoscience*, 5(10), 678–  
582 679, 2012.
- 583 Boulton, A. J.: Conservation of ephemeral streams and their ecosystem services: what are we  
584 missing?: Editorial, *Aquatic Conservation: Marine and Freshwater Ecosystems*, 24(6), 733–738,  
585 doi:10.1002/aqc.2537, 2014.
- 586 Breiman, L.: Random forests, *Machine learning*, 45(1), 5–32, 2001.
- 587 Brugeron, A., Allier, D., Klinka, T.: Approche exploratoire des liens entre référentiels hydrogéologique  
588 et hydrographique : Premières identifications des piézomètres potentiellement représentatifs d'une  
589 relation nappe/rivière et contribution à leur valorisation. Rapport final BRGM/RP-61047-FR. 241 p,  
590 2012.
- 591 Buytaert, W., Zulkafli, Z., Grainger, S., Acosta, L., Alemie, T. C., Bastiaensen, J., De Bièvre, B., Bhusal,  
592 J., Clark, J., Dewulf, A., Foggin, M., Hannah, D. M., Hergarten, C., Isaeva, A., Karpouzoglou, T.,  
593 Pandeya, B., Paudel, D., Sharma, K., Steenhuis, T., Tilahun, S., Van Hecken, G. and Zhumanova, M.:  
594 Citizen science in hydrology and water resources: opportunities for knowledge generation,  
595 ecosystem service management, and sustainable development, *Frontiers in Earth Science*, 2,  
596 doi:10.3389/feart.2014.00026, 2014.
- 597 Clarke, A., Mac Nally, R., Bond, N. and Lake, P. S.: Macroinvertebrate diversity in headwater streams:  
598 a review, *Freshwater Biology*, 53(9), 1707–1721, doi:10.1111/j.1365-2427.2008.02041.x, 2008.
- 599 Costigan, K. H., Jaeger, K. L., Goss, C. W., Fritz, K. M. and Goebel, P. C.: Understanding controls on  
600 flow permanence in intermittent rivers to aid ecological research: integrating meteorology, geology  
601 and land cover: Integrating Science to Understand Flow Intermittence, *Ecohydrology*, 9(7), 1141–  
602 1153, doi:10.1002/eco.1712, 2016.
- 603 Datry, T.: Benthic and hyporheic invertebrate assemblages along a flow intermittence gradient:  
604 effects of duration of dry events: River drying and temporary river invertebrates, *Freshwater Biology*,  
605 57(3), 563–574, doi:10.1111/j.1365-2427.2011.02725.x, 2012.
- 606 Datry, T., Larned, S. T., Fritz, K. M., Bogan, M. T., Wood, P. J., Meyer, E. I. and Santos, A. N.: Broad-  
607 scale patterns of invertebrate richness and community composition in temporary rivers: effects of  
608 flow intermittence, *Ecography*, 37(1), 94–104, doi:10.1111/j.1600-0587.2013.00287.x, 2014a.
- 609 Datry, T., Larned, S. T. and Tockner, K.: Intermittent Rivers: A Challenge for Freshwater Ecology,  
610 *BioScience*, 64(3), 229–235, doi:10.1093/biosci/bit027, 2014b.

- 611 Datry, T., Pella, H., Leigh, C., Bonada, N. and Hugueny, B.: A landscape approach to advance  
612 intermittent river ecology, *Freshwater Biology*, 61(8), 1200–1213, doi:10.1111/fwb.12645, 2016a.
- 613 Datry, T., Fritz, K. and Leigh, C.: Challenges, developments and perspectives in intermittent river  
614 ecology, *Freshwater Biology*, 61(8), 1171–1180, doi:10.1111/fwb.12789, 2016b.
- 615 De Girolamo, A. M., Lo Porto, A., Pappagallo, G., Tzoraki, O. and Gallart, F.: The Hydrological Status  
616 Concept: Application at a Temporary River (Candelaro, Italy): EVALUATING HYDROLOGICAL STATUS  
617 IN TEMPORARY RIVERS, *River Research and Applications*, 31(7), 892–903, doi:10.1002/rra.2786,  
618 2015.
- 619 De Girolamo, A. M., Bouraoui, F., Buffagni, A., Pappagallo, G. and Lo Porto, A.: Hydrology under  
620 climate change in a temporary river system: Potential impact on water balance and flow regime,  
621 *River Research and Applications*, doi:10.1002/rra.3165, 2017a.
- 622 De Girolamo, A. M., Barca, E., Pappagallo, G. and Lo Porto, A.: Simulating ecologically relevant  
623 hydrological indicators in a temporary river system, *Agricultural Water Management*, 180, 194–204,  
624 doi:10.1016/j.agwat.2016.05.034, 2017b.
- 625 Döll, P. and Schmied, H. M.: How is the impact of climate change on river flow regimes related to the  
626 impact on mean annual runoff? A global-scale analysis, *Environmental Research Letters*, 7(1),  
627 014037, doi:10.1088/1748-9326/7/1/014037, 2012.
- 628 Eng, K., Wolock, D. M. and Dettinger, M. D.: Sensitivity of Intermittent Streams to Climate Variations  
629 in the USA: Sensitivity of Intermittent Streams, *River Research and Applications*, 32(5), 885–895,  
630 doi:10.1002/rra.2939, 2016.
- 631 Finn, D. S., Bonada, N., M?rria, C. and Hughes, J. M.: Small but mighty: headwaters are vital to stream  
632 network biodiversity at two levels of organization, *Journal of the North American Benthological*  
633 *Society*, 30(4), 963–980, doi:10.1899/11-012.1, 2011.
- 634 Fritz, K. M., Hagenbuch, E., D'Amico, E., Reif, M., Wigington, P. J., Leibowitz, S. G., Comeleo, R. L.,  
635 Ebersole, J. L. and Nadeau, T.-L.: Comparing the Extent and Permanence of Headwater Streams From  
636 Two Field Surveys to Values From Hydrographic Databases and Maps, *JAWRA Journal of the*  
637 *American Water Resources Association*, 49(4), 867–882, doi:10.1111/jawr.12040, 2013.
- 638 Gallart, F., Prat, N., García-Roger, E. M., Latron, J., Rieradevall, M., Llorens, P., Barberá, G. G., Brito,  
639 D., De Girolamo, A. M., Lo Porto, A., Buffagni, A., Erba, S., Neves, R., Nikolaidis, N. P., Perrin, J. L.,  
640 Querner, E. P., Quiñonero, J. M., Tournoud, M. G., Tzoraki, O., Skoulikidis, N., Gómez, R., Sánchez-  
641 Montoya, M. M. and Froebrich, J.: A novel approach to analysing the regimes of temporary streams  
642 in relation to their controls on the composition and structure of aquatic biota, *Hydrology and Earth*  
643 *System Sciences*, 16(9), 3165–3182, doi:10.5194/hess-16-3165-2012, 2012.
- 644 Gallart, F., Llorens, P., Latron, J., Cid, N., Rieradevall, M. and Prat, N.: Validating alternative  
645 methodologies to estimate the regime of temporary rivers when flow data are unavailable, *Science*  
646 *of The Total Environment*, 565, 1001–1010, doi:10.1016/j.scitotenv.2016.05.116, 2016.
- 647 Garcia, C., Gibbins, C. N., Pardo, I. and Batalla, R. J.: Long term flow change threatens invertebrate  
648 diversity in temporary streams: Evidence from an island, *Science of The Total Environment*, 580,  
649 1453–1459, doi:10.1016/j.scitotenv.2016.12.119, 2017a.

650 Garcia, C., Amengual, A., Homar, V. and Zamora, A.: Losing water in temporary streams on a  
651 Mediterranean island: Effects of climate and land-cover changes, *Global and Planetary Change*, 148,  
652 139–152, doi:10.1016/j.gloplacha.2016.11.010, 2017b.

653 Gómez, R., Hurtado, I., Suárez, M. L. and Vidal-Abarca, M. R.: Ramblas in south-east Spain:  
654 threatened and valuable ecosystems, *Aquatic Conservation* 15, 387–402, doi:10.1002/aqc.680, 2005.

655 González-Ferreras, A. M. and Barquín, J.: Mapping the temporary and perennial character of whole  
656 river networks: MAPPING FLOW PERMANENCE IN RIVER NETWORK, *Water Resources Research*,  
657 doi:10.1002/2017WR020390, 2017.

658 Huxter, E. H. H. and (Ilja) van Meerveld, H. J.: Intermittent and Perennial Streamflow Regime  
659 Characteristics in the Okanagan, *Canadian Water Resources Journal / Revue canadienne des*  
660 *ressources hydriques*, 37(4), 391–414, doi:10.4296/cwrj2012-910, 2012.

661 Jaeger, K. L., Olden, J. D. and Pelland, N. A.: Climate change poised to threaten hydrologic  
662 connectivity and endemic fishes in dryland streams, *Proceedings of the National Academy of*  
663 *Sciences*, 111(38), 13894–13899, doi:10.1073/pnas.1320890111, 2014.

664 Kelso, J. E. and Entekin, S. A.: Intermittent and perennial macroinvertebrate communities had similar  
665 richness but differed in species trait composition depending on flow duration, *Hydrobiologia*, 807(1),  
666 189–206, doi:10.1007/s10750-017-3393-y, 2018.

667 Larned, S. T., Datry, T., Arscott, D. B. and Tockner, K.: Emerging concepts in temporary-river ecology,  
668 *Freshwater Biology*, 55(4), 717–738, doi:10.1111/j.1365-2427.2009.02322.x, 2010.

669 Lee, S.: Application of logistic regression model and its validation for landslide susceptibility mapping  
670 using GIS and remote sensing data, *International Journal of Remote Sensing*, 26(7), 1477–1491,  
671 doi:10.1080/01431160412331331012, 2005.

672 Leigh, C. and Datry, T.: Drying as a primary hydrological determinant of biodiversity in river systems:  
673 a broad-scale analysis, *Ecography*, 40(4), 487–499, doi:10.1111/ecog.02230, 2017.

674 Leigh, C., Boulton, A. J., Courtwright, J. L., Fritz, K., May, C. L., Walker, R. H. and Datry, T.: Ecological  
675 research and management of intermittent rivers: an historical review and future directions,  
676 *Freshwater Biology*, 61(8), 1181–1199, doi:10.1111/fwb.12646, 2016.

677 Leopold, L. B.: *A View of the River*. Harvard University Press, Cambridge, Massachusetts, USA, 1994.

678 Leopold, L. B., Wolman, M. G. and Miller, J. P.: *Fluvial Processes in Geomorphology*. Dover  
679 Publications, New York, USA, 1964.

680 Meyer, J. L., Strayer, D. L., Wallace, J. B., Eggert, S. L., Helfman, G. S. and Leonard, N. E.: The  
681 Contribution of Headwater Streams to Biodiversity in River Networks<sup>1</sup>: The Contribution of  
682 Headwater Streams to Biodiversity in River Networks, *JAWRA Journal of the American Water*  
683 *Resources Association*, 43(1), 86–103, doi:10.1111/j.1752-1688.2007.00008.x, 2007.

684 Nadeau, T.-L. and Rains, M. C.: Hydrological Connectivity Between Headwater Streams and  
685 Downstream Waters: How Science Can Inform Policy<sup>1</sup>: Hydrological Connectivity Between  
686 Headwater Streams and Downstream Waters: How Science Can Inform Policy, *JAWRA Journal of the*  
687 *American Water Resources Association*, 43(1), 118–133, doi:10.1111/j.1752-1688.2007.00010.x,  
688 2007.

- 689 Nash, J. E. and Sutcliffe, J. V.: River flow forecasting through conceptual models part I — A discussion  
690 of principles, *Journal of Hydrology*, 10(3), 282–290, doi:10.1016/0022-1694(70)90255-6, 1970.
- 691 Nowak, C. and Durozoi, B.: Observatoire National Des Etiages, Note technique, ONEMA., 2012.
- 692 Pella, H., Lejot, J., Lamouroux, N. and Snelder, T.: Le réseau hydrographique théorique (RHT) français  
693 et ses attributs environnementaux, *Géomorphologie: relief, processus, environnement*, 18(3), 317–  
694 336, 2012.
- 695 Pumo, D., Caracciolo, D., Viola, F. and Noto, L. V.: Climate change effects on the hydrological regime  
696 of small non-perennial river basins, *Science of The Total Environment*, 542, 76–92,  
697 doi:10.1016/j.scitotenv.2015.10.109, 2016.
- 698 Reynolds, L. V., Shafroth, P. B. and LeRoy Poff, N.: Modeled intermittency risk for small streams in the  
699 Upper Colorado River Basin under climate change, *Journal of Hydrology*, 523, 768–780,  
700 doi:10.1016/j.jhydrol.2015.02.025, 2015.
- 701 Sarremejane, R., Cañedo-Argüelles, M., Prat, N., Mykrä, H., Muotka, T. and Bonada, N.: Do  
702 metacommunities vary through time? Intermittent rivers as model systems, *Journal of Biogeography*,  
703 44(12), 2752–2763, doi:10.1111/jbi.13077, 2017.
- 704 Sauquet, E., Gottschalk, L. and Krasovskaia, I.: Estimating mean monthly runoff at ungauged  
705 locations: an application to France, *Hydrology Research*, 39(5–6), 403, doi:10.2166/nh.2008.331,  
706 2008.
- 707 Skoulikidis, N. T.: The environmental state of rivers in the Balkans—A review within the DPSIR  
708 framework, *Science of The Total Environment*, 407(8), 2501–2516,  
709 doi:10.1016/j.scitotenv.2009.01.026, 2009.
- 710 Skoulikidis, N. T., Vardakas, L., Karaouzas, I., Economou, A. N., Dimitriou, E. and Zogaris, S.: Assessing  
711 water stress in Mediterranean lotic systems: insights from an artificially intermittent river in Greece,  
712 *Aquatic Sciences*, 73(4), 581–597, doi:10.1007/s00027-011-0228-1, 2011.
- 713 Skoulikidis, N. T., Vardakas, L., Amaxidis, Y. and Michalopoulos, P.: Biogeochemical processes  
714 controlling aquatic quality during drying and rewetting events in a Mediterranean non-perennial river  
715 reach, *Science of The Total Environment*, 575, 378–389, doi:10.1016/j.scitotenv.2016.10.015, 2017a.
- 716 Skoulikidis, N. T., Sabater, S., Datry, T., Morais, M. M., Buffagni, A., Dörflinger, G., Zogaris, S., del Mar  
717 Sánchez-Montoya, M., Bonada, N., Kalogianni, E., Rosado, J., Vardakas, L., De Girolamo, A. M. and  
718 Tockner, K.: Non-perennial Mediterranean rivers in Europe: Status, pressures, and challenges for  
719 research and management, *Science of The Total Environment*, 577, 1–18,  
720 doi:10.1016/j.scitotenv.2016.10.147, 2017b.
- 721 Snelder, T. H., Datry, T., Lamouroux, N., Larned, S. T., Sauquet, E., Pella, H. and Catalogne, C.:  
722 Regionalization of patterns of flow intermittence from gauging station records, *Hydrology and Earth  
723 System Sciences*, 17(7), 2685–2699, doi:10.5194/hess-17-2685-2013, 2013.
- 724 Storey, R. G. and Quinn, J. M.: Survival of aquatic invertebrates in dry bed sediments of intermittent  
725 streams: temperature tolerances and implications for riparian management, *Freshwater Science*,  
726 32(1), 250–266, doi:10.1899/12-008.1, 2013.

727 Stubbington, R. and Datry, T.: The macroinvertebrate seedbank promotes community persistence in  
728 temporary rivers across climate zones, *Freshwater Biology*, 58(6), 1202–1220,  
729 doi:10.1111/fwb.12121, 2013.

730 Turner, D. S. and Richter, H. E.: Wet/Dry Mapping: Using Citizen Scientists to Monitor the Extent of  
731 Perennial Surface Flow in Dryland Regions, *Environmental Management*, 47(3), 497–505,  
732 doi:10.1007/s00267-010-9607-y, 2011.

733 Vadher, A. N., Millett, J., Stubbington, R. and Wood, P. J.: Drying duration and stream characteristics  
734 influence macroinvertebrate survivorship within the sediments of a temporary channel and exposed  
735 gravel bars of a connected perennial stream, *Hydrobiologia*, doi:10.1007/s10750-018-3544-9, 2018.

736 van Meerveld, H. J. I., Vis, M. J. P. and Seibert, J.: Information content of stream level class data for  
737 hydrological model calibration, *Hydrology and Earth System Sciences*, 21(9), 4895–4905,  
738 doi:10.5194/hess-21-4895-2017, 2017.

739 Vardakas, L., Kalogianni, E., Economou, A. N., Koutsikos, N. and Skoulikidis, N. T.: Mass mortalities  
740 and population recovery of an endemic fish assemblage in an intermittent river reach during drying  
741 and rewetting, *Fundamental and Applied Limnology / Archiv für Hydrobiologie*,  
742 doi:10.1127/fal/2017/1056, 2017.

743 Wasson, J.-G., Chandesris, A., Pella, H. and Blanc, L.: Typology and reference conditions for surface  
744 water bodies in France: the hydro-ecoregion approach, *TemaNord*, 566, 37–41, 2002.

745 Woelfle-Erskine, C.: Collaborative Approaches to Flow Restoration in Intermittent Salmon-Bearing  
746 Streams: Salmon Creek, CA, USA, *Water*, 9(3), 217, doi:10.3390/w9030217, 2017.

747

748

	Stations with at least one drying event	Stations with drying > 50%	Frequency of discharge < 1 l/s
<b>2012</b>	79	19	32.7
<b>2013</b>	47	14	37.9
<b>2014</b>	54	15	32.9
<b>2015</b>	76	21	31.1
<b>2016</b>	71	19	28.6

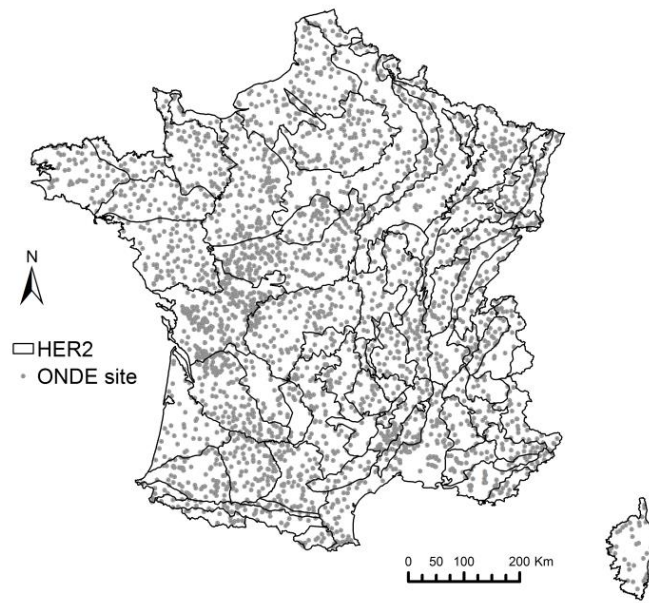
749 **Table 1.** Annual statistics on flow intermittence calculated on HYDRO gauging stations between the  
750 1<sup>st</sup> May and the 30<sup>th</sup> September

751

		2011-2017 dataset						1989-2017 dataset					
		Calibration					Valid.	Calibration					Valid.
		2012	2013	2014	2015	2016	2017	2012	2013	2014	2015	2016	2017
LLR model	May	0.2	0.0	0.5	0.5	0.6	<b>0.4</b>	0.2	0.0	0.3	0.0	0.7	<b>0.2</b>
	June	0.6	0.3	0.8	0.5	0.8	<b>0.5</b>	0.6	0.3	0.5	0.3	0.8	<b>0.5</b>
	July	0.7	0.5	0.6	0.6	0.8	<b>0.7</b>	0.7	0.5	0.5	0.4	0.8	<b>0.6</b>
	August	0.8	0.6	0.7	0.7	0.8	<b>0.6</b>	0.7	0.5	0.5	0.5	0.8	<b>0.6</b>
	Sept.	0.7	0.8	0.6	0.6	0.7	<b>0.6</b>	0.6	0.7	0.5	0.5	0.6	<b>0.6</b>
	May - Sept	0.8	0.8	0.7	0.7	0.8	<b>0.7</b>	0.8	0.7	0.5	0.6	0.8	<b>0.7</b>
LR model	May	0.2	0.0	0.5	0.1	0.6	<b>0.3</b>	0.3	0.0	0.3	0.0	0.7	<b>0.2</b>
	June	0.6	0.5	0.8	0.5	0.8	<b>0.4</b>	0.6	0.4	0.5	0.3	0.7	<b>0.4</b>
	July	0.7	0.6	0.5	0.6	0.8	<b>0.6</b>	0.7	0.4	0.5	0.4	0.8	<b>0.6</b>
	August	0.7	0.6	0.7	0.6	0.7	<b>0.6</b>	0.6	0.4	0.5	0.4	0.7	<b>0.5</b>
	Sept.	0.6	0.8	0.6	0.7	0.7	<b>0.6</b>	0.5	0.6	0.4	0.5	0.6	<b>0.6</b>
	May - Sept	0.8	0.8	0.7	0.7	0.8	<b>0.7</b>	0.8	0.7	0.5	0.6	0.8	<b>0.7</b>

752 **Table 2.** NSE criteria obtained between 2012 and 2017 with the LLR and LR models calibrated over  
753 the period 2012-2016.

754



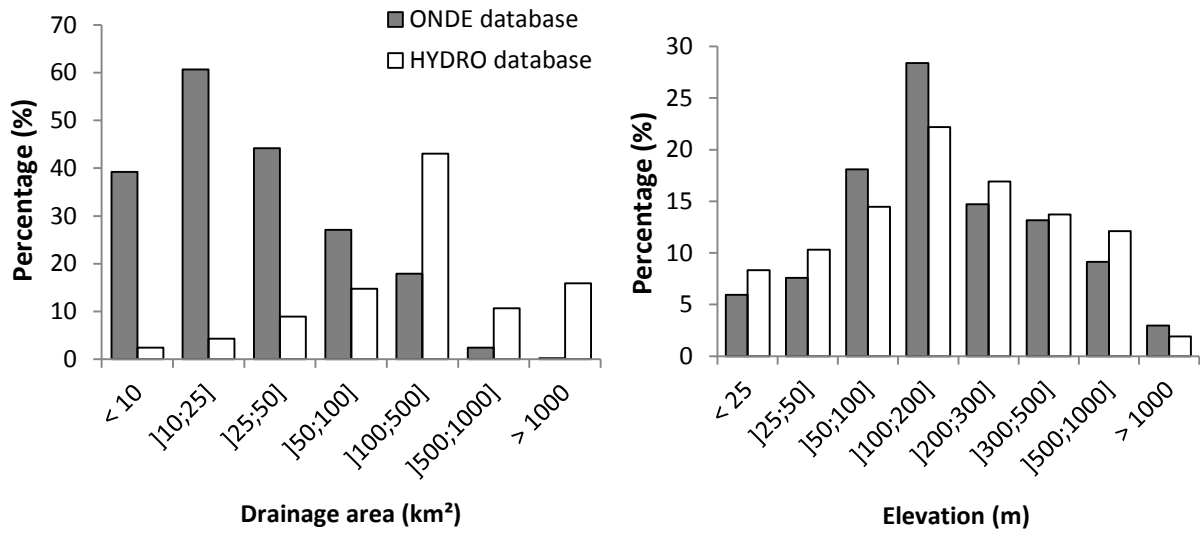
755

756

**Figure 1.** Location of the 3300 ONDE sites and partition into HER2.

757





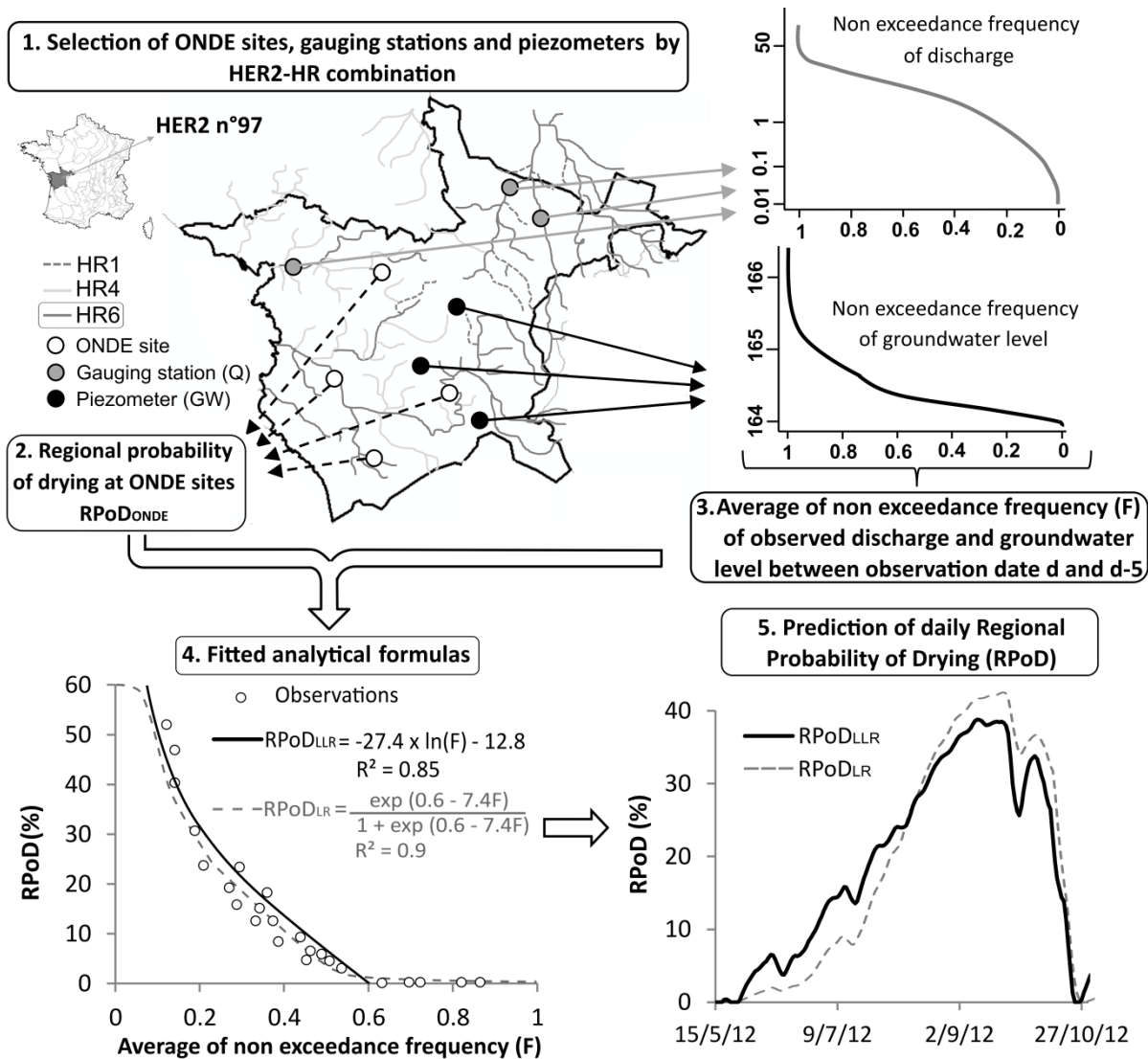
758

759

760

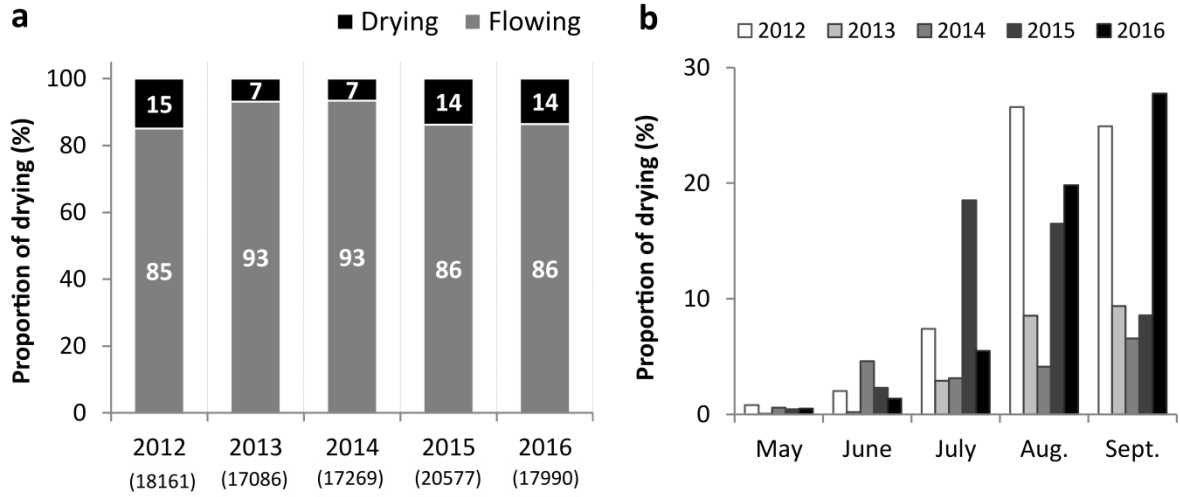
761

**Figure 2.** Distribution of the 3 300 ONDE sites and of the 1 600 gauging stations available in the HYDRO database against: (a) drainage area and (b) elevation.



762  
 763  
 764  
 765

**Figure 3.** Strategy of parametric modeling (step 1-4) developed to predict (step 5) the regional probability of drying (RPoD) by HER2-HR combination in France.



766

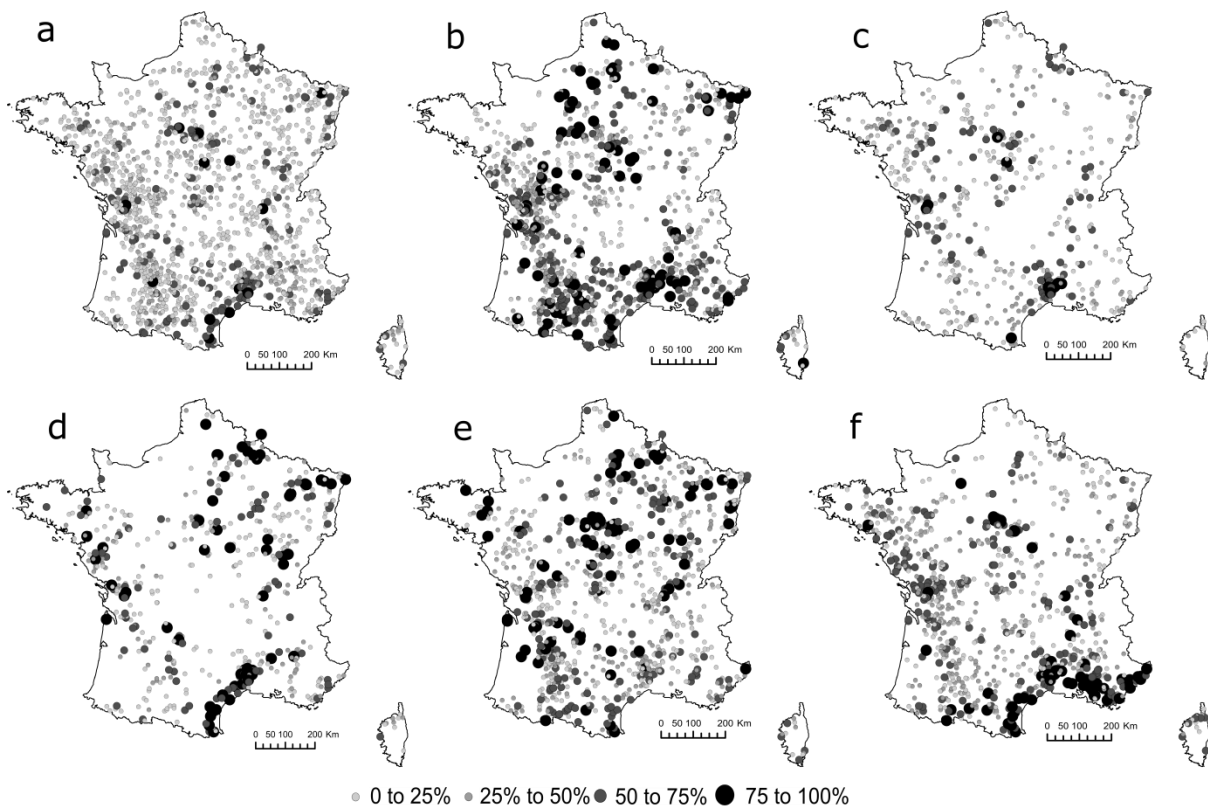
767

768

769

770

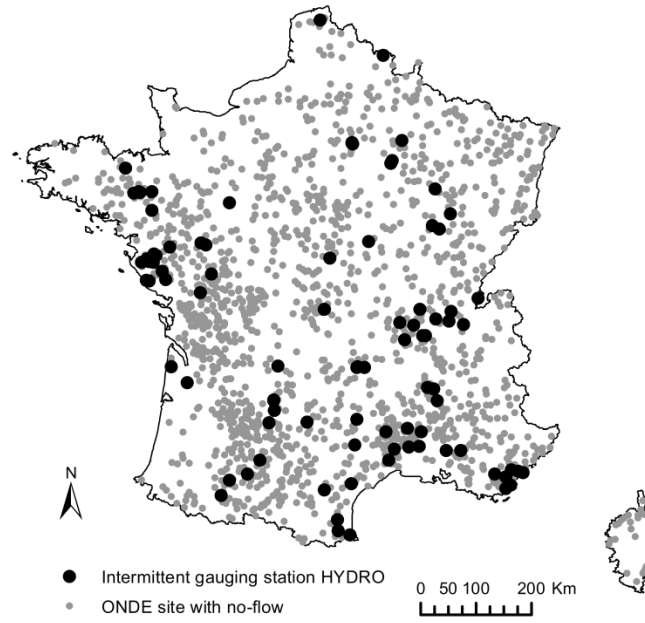
**Figure 4.** (a) Distribution of yearly proportion of drying observed with the ONDE network with the total yearly number of ONDE observations written in brackets and (b) distribution of proportions of drying per year and per month.



771

772 **Figure 5.** Distribution of the percentages of drying observed at ONDE sites for the years: (a) 2012-  
 773 2016, (b) 2012, (c) 2013, (d) 2014, (e) 2015 and (f) 2016.

774

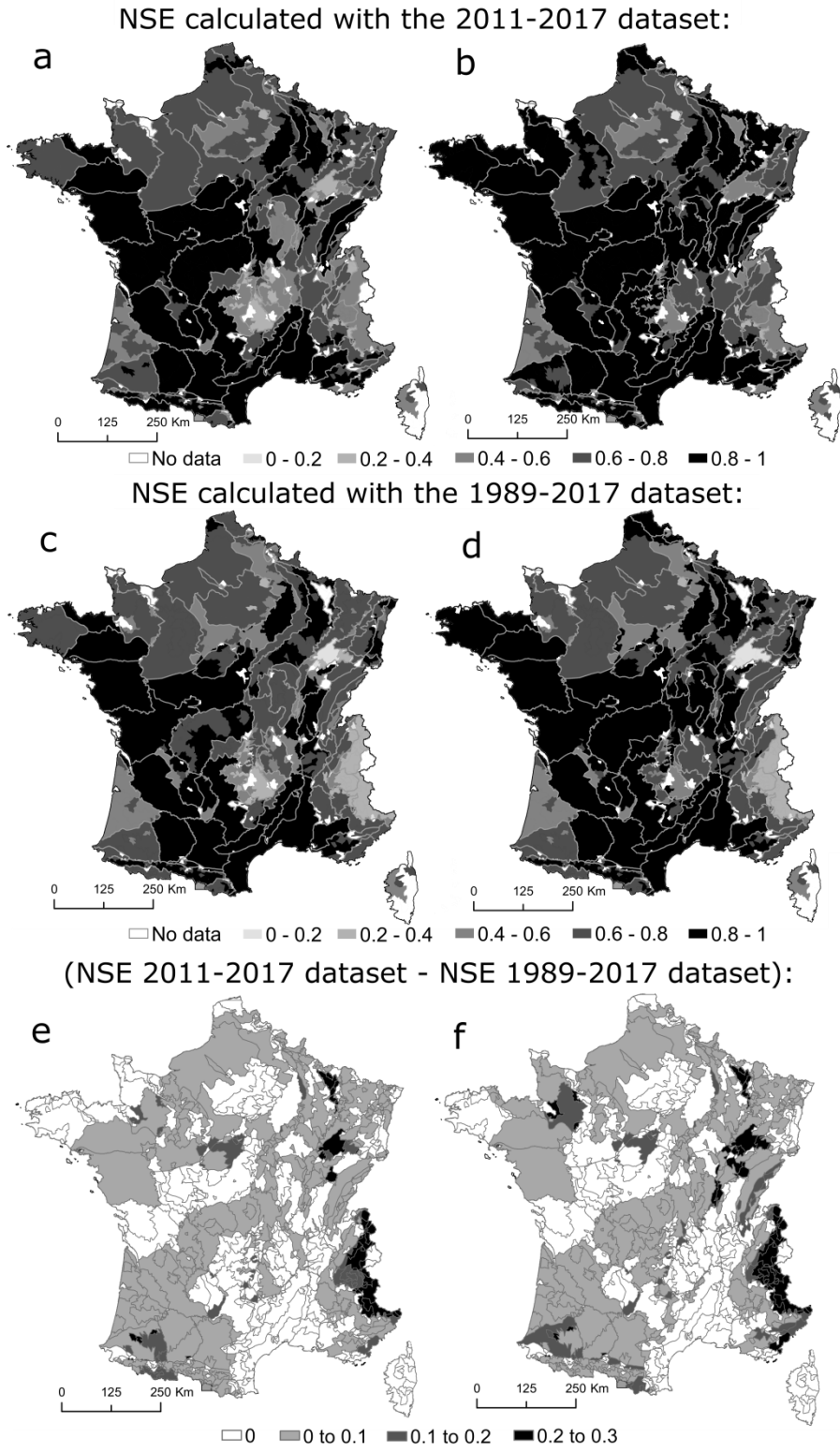


775

776

**Figure 6.** Map of ONDE sites and HYDRO gauging stations having at least one drying.

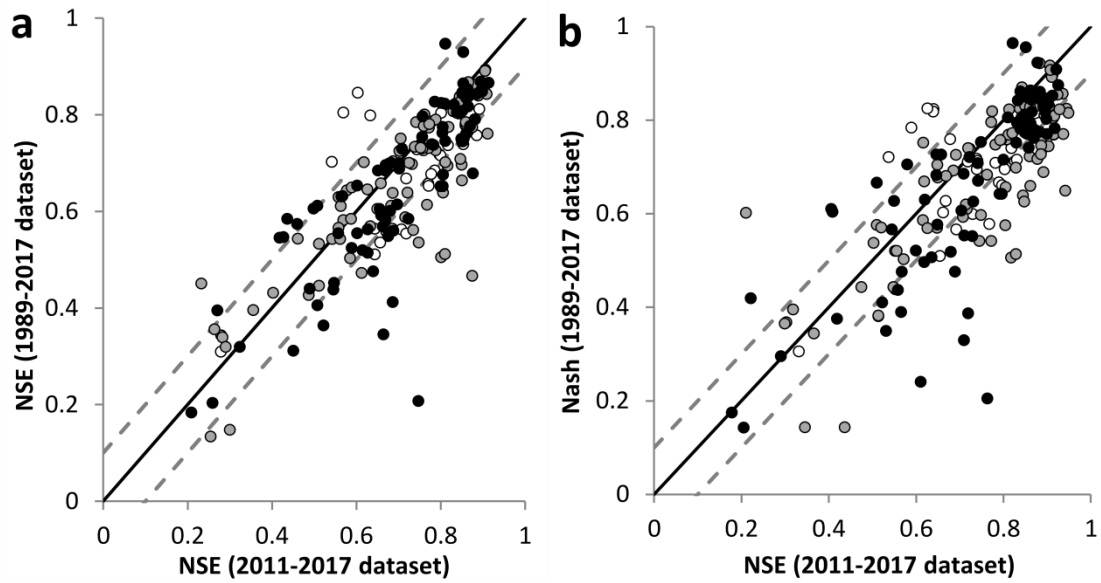
777



778

779 **Figure 7.** Map of Nash-Sutcliffe criteria (NSE) obtained for each HER2-HR combination between 2012  
 780 and 2016 with the 2011-2017 and 1989-2017 datasets according to: (a) and (c) a log-linear regression  
 781 (LLR) model; (b) and (d) a logistic regression (LR) model. NSE differences between the 2011-2017  
 782 dataset and the 1989-2017 dataset are represented for: (e) LLR model and (f) LR model.

783

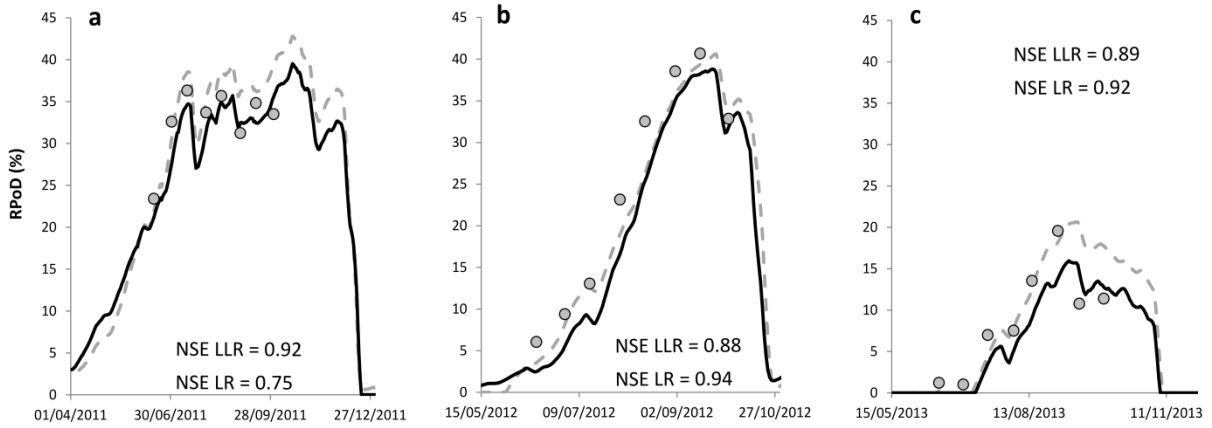


784

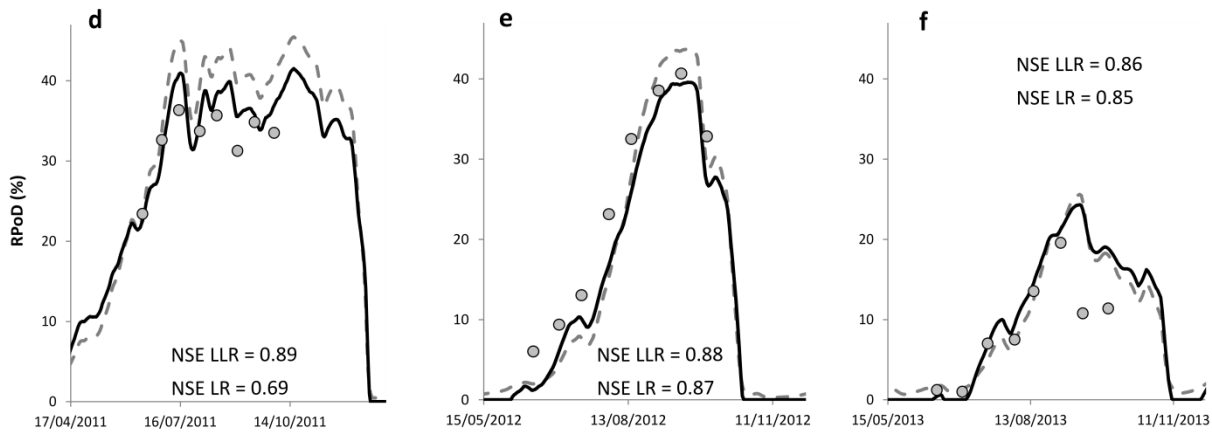
785 **Figure 8.** NSE calculated for each HER2-HR combination between 2012 and 2016 with the 1989-2017  
 786 dataset as a function of NSE calculated with 2011-2017 dataset with respectively: (a) the LLR model  
 787 and (b) the LR model. The color of dots represents the proportion of gauging station and piezometers  
 788 lost between the 2011-2017 database and the 1989-2017 database: losses < 50% (white); losses  
 789 between 50% and 75% (grey); losses > 75% (black).

790

RPoD simulated with the 2011-2017 dataset:



RPoD simulated with the 1989-2017 dataset:



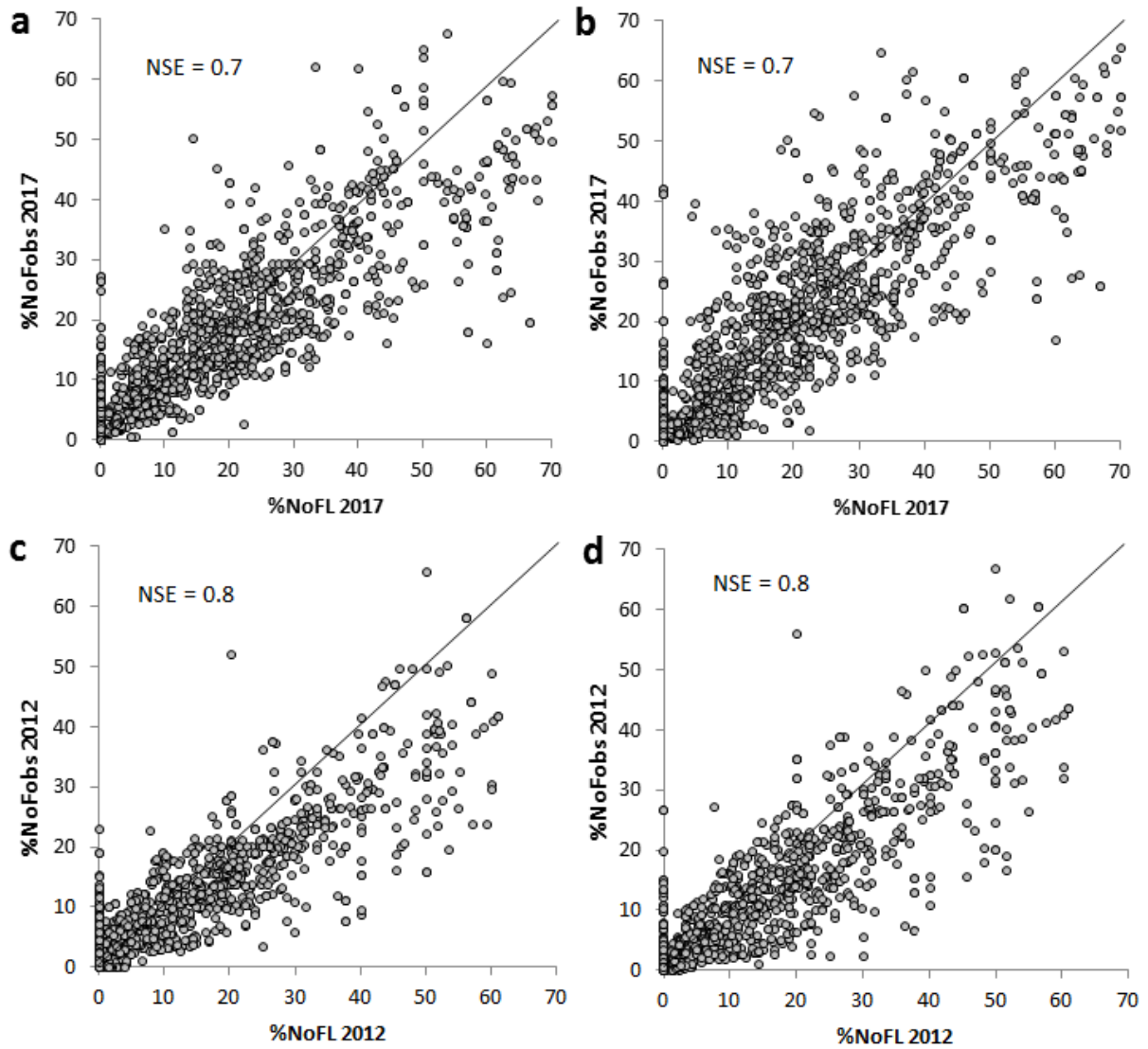
— LLR model    - - - - LR model    ● Obs - POC data

791

792 **Figure 9.** Comparison between observed proportion of drying  $RPoD_{POC}$  and RPoD predicted by the LLR  
 793 and LR models with the 2011-2017 dataset in: (a) 2011, (b) 2012 (c) 2013 and with the 1989-2017  
 794 dataset in: (d) 2011, (e) 2012 (f) 2013.

795

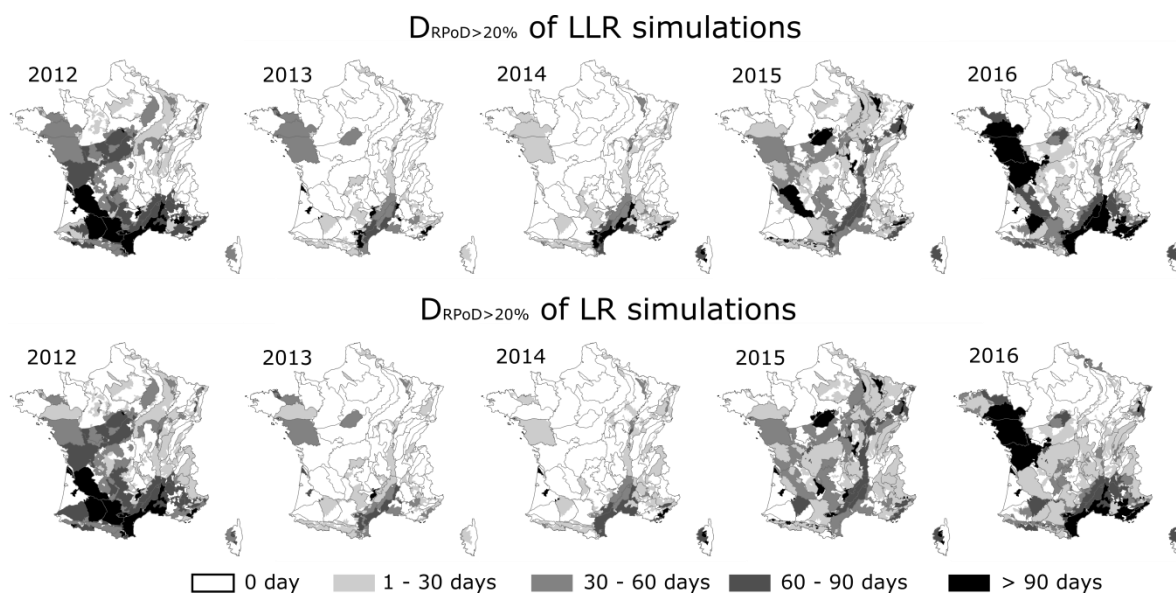




796

797 **Figure 10.** Scatter plot of the predicted RPoD (x axis) and drying observed at ONDE sites (y axis) in  
 798 2017 and 2012 simulated with the 2011-2017 dataset by: (a) and (c) the LLR model and (b) and (d)  
 799 the LR model.

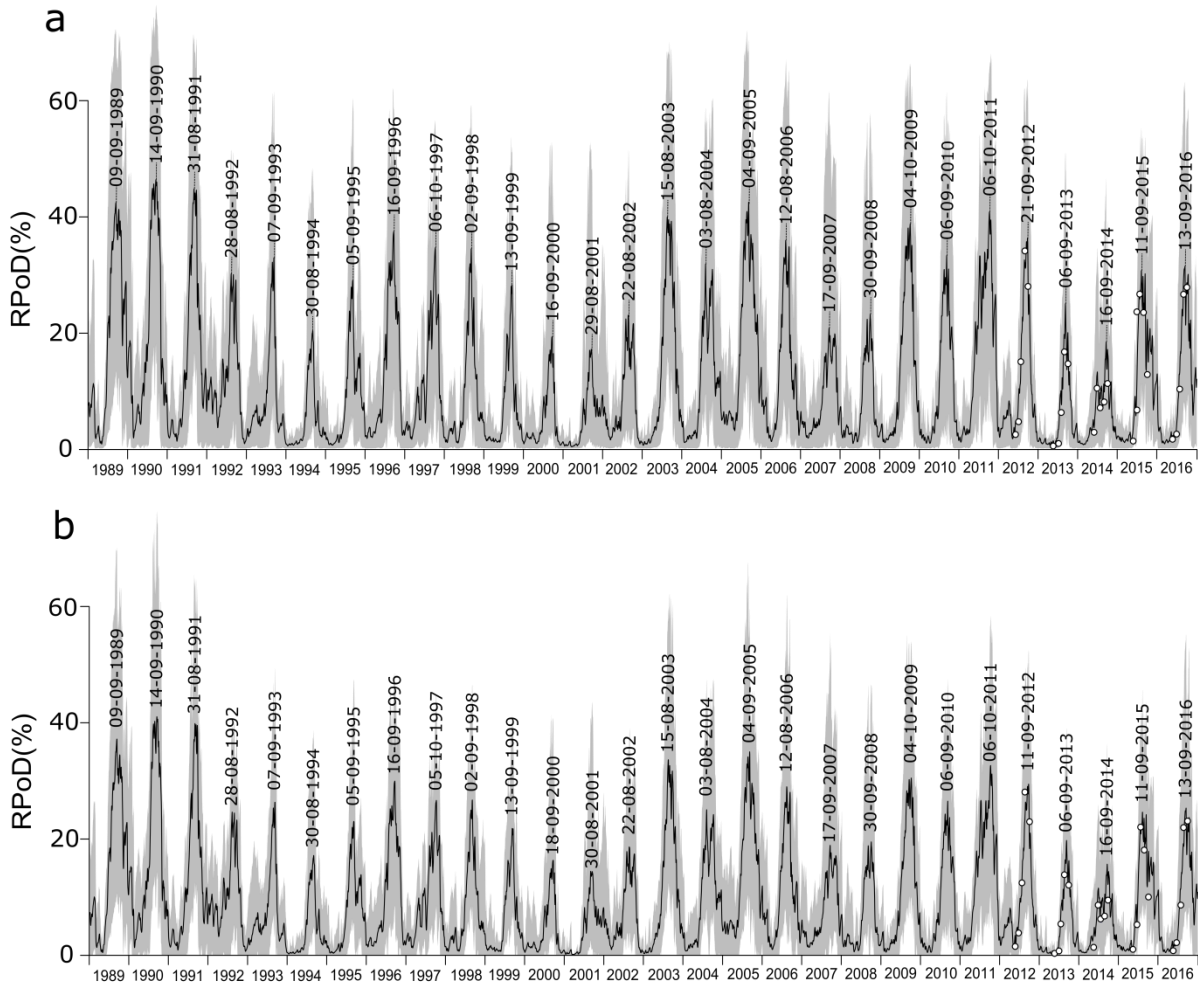
800



801

802 **Figure 11.** Maximum duration of consecutive days with RPoD higher than 20% simulated with LLR  
 803 and LR model.

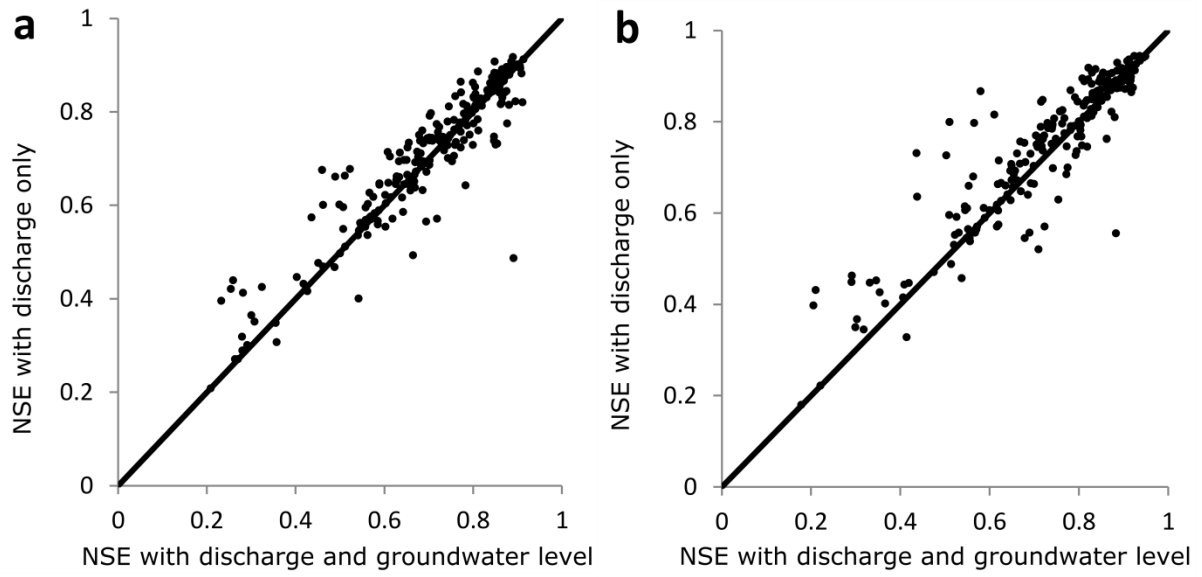
804



805

806 **Figure 12.** RPOD simulated between 1989 and 2016 the 1989-2017 dataset with: (a) the LR model and  
 807 (b) the LLR model. The grey area represents the RPOD between the 90<sup>th</sup> percentile and the 10<sup>th</sup>  
 808 percentile simulated on HER2-HR combination, the black curve represents the average RPOD  
 809 simulated by HER2-HR combination and white dots represent the mean RPOD<sub>ONDE</sub> for each  
 810 observation dates. Dates mentioned correspond to the day of the maximum average RPOD simulated  
 811 by HER2-HR combination (black curve) of each year.

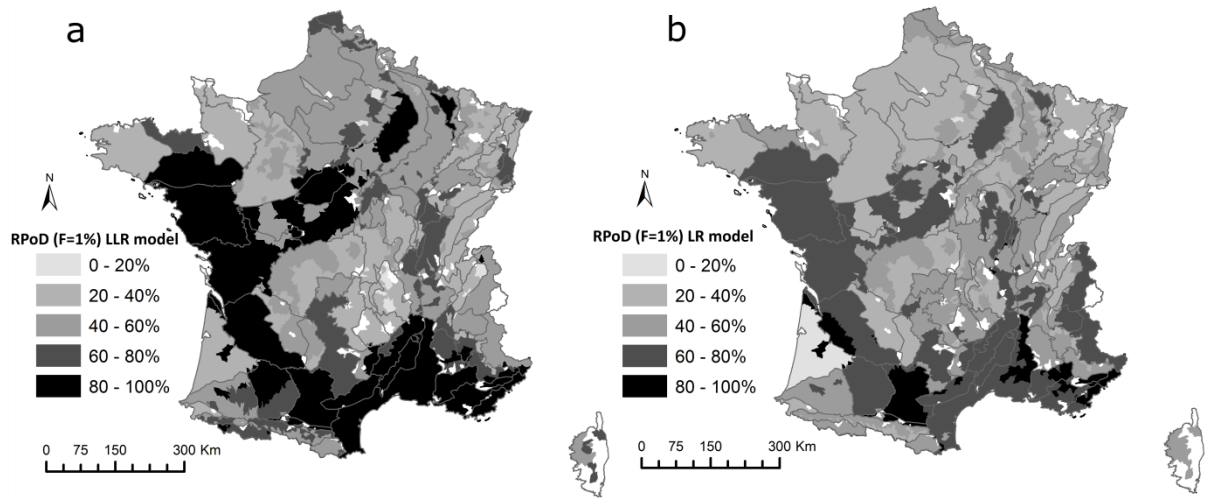
812



813

814 **Figure 13.** Comparison of NSE obtained with regression including only discharge variable as a  
 815 function of NSE obtained with including discharge and groundwater level variables in the 2011-2017  
 816 dataset with: (a) LLR model and (b) LR model.

817



818

819 **Figure 14.** Regional probability of drying simulated with F = 1% predicted with: (a) the LLR model and  
 820 (b) the LR model.

821

822

823

824

825

826

827

828

829

830

831